Stochastic thermodynamics of an electron spin resonance quantum dot system

JunYan Luo,[1,*] Yiying Yan,[1] Hailong Wang,[1] Jing Hu,[1] Xiao-Ling He,[1] and Gernot Schaller[2]
[1]*Department of Physics, Zhejiang University of Science and Technology, Hangzhou 310023, China*
[2]*Institut für Theoretische Physik, Technische Universität Berlin, Hardenbergstrasse 36, D-10623 Berlin, Germany*

(Received 28 October 2019; revised manuscript received 7 February 2020; accepted 18 February 2020; published 10 March 2020)

We present a stochastic thermodynamics analysis of an electron spin resonance pumped quantum dot device in the Coulomb-blocked regime, where a pure spin current is generated without an accompanying net charge current. Based on a generalized quantum master equation beyond secular approximation, quantum coherences are accounted for in terms of an average spin in the Floquet basis. Elegantly, this average spin undergoes a precession about an effective magnetic field, which originates from the nonsecular treatment and energy renormalization. It is shown that the interaction between average spin and effective magnetic field may have the dominant roles to play in both energy transport and irreversible entropy production. In the stationary limit, the energy and entropy balance relations are also established based on the theory of counting statistics.

DOI: 10.1103/PhysRevB.101.125410

I. INTRODUCTION

The state-of-the-art nanofabrication is able to create small systems far from the thermodynamic limit, where both thermal and quantum mechanical fluctuations have essential roles to play. This opens up opportunities to create new functional devices but also poses great challenges to manipulate nanoscale systems, which interact with their environments and exchange energy in a random manner [1]. Understanding thermodynamics from quantum mechanics [2–11] is thus of fundamental significance to characterize energy fluctuations at the microscopic level and also of technological importance for the design of efficient quantum heat engines [12–20] and exploration of information processing capabilities [21–30].

In comparison with a soft-matter system, where fluctuation relations were first measured experimentally [31], a solid-state device is considered to be an ideal testbed to investigate thermodynamics of open quantum systems due to a number of intriguing advantages [32,33]. For instance, solid-state systems are robust such that experiments can be repeated normally up to a million times under the same conditions. Moreover, the particles and quantum states, as well as their couplings to the environments, can be manipulated in a precise way. Measurement of the statistics of the dissipated energy has been proven to satisfy the Jarzynski equality and Crooks fluctuation relations [34]. Furthermore, the generalized Jarzynski equality has also been validated in a double-dot Szilard engine under feedback control [35]. So far, experimentalists have been able to implement a quantum Maxwell demon either in a superconducting circuit [36,37] or in a single electron box [38], where the intimate relation between work and information is unambiguously revealed.

Recent progress in solid-state engineering has made it possible to control spin coherence to the timescale of seconds [39,40], thus ushering in a new era of ultracoherent spintronics [41,42]. This provides an exciting opportunity to incorporate spintronics into thermodynamics and evaluate both energetic and entropic costs to manipulate spin information. In contrast to a conventional electronic setup, where information and energy are transmitted via charge, in a spintronic device it is the spin that will work as a vehicle for energy and information transduction. However, different from the charge, which is conserved as an electron moves from one place to another, the orientation of the spin, as an intrinsic angular momentum, is not invariant in transport [41]. It is therefore essential to explore the energy and entropy balance relations in terms of a pure spin current without accompanying a charge current and understand what kind of roles the dynamics of spin will play in these processes.

This work is devoted to unveil the underlying mechanisms by analyzing the stochastic thermodynamics of an electron spin resonance (ESR) pumped quantum dot (QD) system in the Coulomb-blockaded regime, where a pure spin current is generated without a net charge flow. Based on a generalized quantum master equation (GQME) beyond secular approximation, the effect of coherences is taken into account via an average spin, which builds up and decays due to tunnel coupling to an electrode. Remarkably, the nonsecular treatment and energy renormalization give rise to an effective magnetic field, about which the average spin undergoes precession. It is revealed that, under the circumstance of strong asymmetry in spin tunneling, the interaction between average spin and effective magnetic field play the dominant roles in energy flow as well as in the irreversible entropy production.

This paper is organized as follows. We begin in Sec. II with an introduction of the ESR pumped QD system, where a pure spin current is generated without accompanying a net charge current. The GQME is derived in Sec. III, with special attention paid to the unique influence of nonsecular treatment on the spin dynamics and spin current. In particular, the quantum coherences are revealed to have vital roles to play in energy

*jyluo@zust.edu.cn

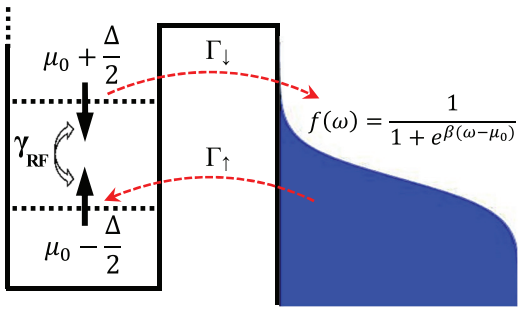

FIG. 1. A schematic of an ESR pumped QD system, where a single QD is tunnel coupled to a side electron reservoir characterized by the Fermi function $f(\omega)$, with inverse temperature $\beta = (k_B T)^{-1}$ and chemical potential μ_0 located in the middle of the spin-up ($\mu_0 - \frac{\Delta}{2}$) and spin-down ($\mu_0 + \frac{\Delta}{2}$) levels. The ESR pumping produces a pure spin current in the absence of a net charge current.

current. Section IV is devoted to the analysis of stochastic thermodynamics based on the counting statistics, where both energy balance and entropy balance relations are established. Furthermore, the influence of the interaction between average spin and magnetic field on irreversible entropy production is revealed. Finally, we summarize the work in Sec. V.

II. MODEL DESCRIPTION

We investigate an ESR pumped system closely related to experiments [43,44]. The system is comprised of a Coulomb-blockaded single QD, tunnel coupled to a side electron reservoir (Fig. 1). The QD is exposed to a local external rotating magnetic field

$$\boldsymbol{B} = \{B_\parallel \cos\Omega t, B_\parallel \sin\Omega t, B_\perp\}, \tag{1}$$

where its z component leads to the Zeeman splitting of the single level $\Delta = g_z \mu_B B_\perp$, with g_z the electron g factor in the z direction and μ_B the Bohr magneton. The x and y components of the magnetic field are oscillating in time, where the frequency Ω is tuned very close to Δ, resulting in the well-known ESR and spin flipping in QD. The electron spin is further tunnel coupled to a side reservoir, whose chemical potential μ_0 is set in the middle of the split spin-up and spin-down levels. A spin-up electron may tunnel into QD, where it is pumped to the higher level with its spin orientation flipped and finally tunnels out to the side reservoir. At sufficiently low temperatures, this generates an ESR-pumped spin current without accompanying a net charge current. The Hamiltonian of the total (T) system reads

$$H_T(t) = H_S(t) + H_B + V. \tag{2}$$

The first term describes the QD with ESR pumping

$$H_S(t) = \frac{\Delta}{2}(d_\downarrow^\dagger d_\downarrow - d_\uparrow^\dagger d_\uparrow) + U_C d_\uparrow^\dagger d_\uparrow d_\downarrow^\dagger d_\downarrow + \gamma_{RF}(d_\uparrow^\dagger d_\downarrow e^{i\Omega t} + d_\downarrow^\dagger d_\uparrow e^{-i\Omega t}), \tag{3}$$

where $d_\sigma^\dagger$ and d_σ are the creation and annihilation operators of an electron with spin $\sigma = \{\uparrow, \downarrow\}$ in the QD. Spin-up and spin-down states are coupled to each other due to the rotating magnetic field, with the ESR Rabi frequency given by $\gamma_{RF} = g_\parallel \mu_B B_\parallel$ and $g_\parallel$ the electron g factor perpendicular to z. We stress that in the following we will consider the Coulomb-blockaded limit $U_C \to \infty$, thus effectively forbidding the double occupancy of the QD.

The second term in Eq. (2) depicts the side electron reservoir, which is modeled as a collection of noninteracting electrons

$$H_B = \sum_\sigma H_B^{(\sigma)} = \sum_\sigma \left\{ \sum_k \varepsilon_{k\sigma} c_{k\sigma}^\dagger c_{k\sigma} \right\}, \tag{4}$$

where $H_B^{(\sigma)}$ is defined implicitly, with $c_{k\sigma}^\dagger$ ($c_{k\sigma}$) the creation (annihilation) operator for an electron with momentum k and spin σ. For later use, we also introduce the operator for the number of spin-σ electrons in the electron reservoir

$$N_B^{(\sigma)} = \sum_k c_{k\sigma}^\dagger c_{k\sigma}, \tag{5}$$

such that the operator for the total number of electrons in the reservoir is $N_B = \sum_\sigma N_B^{(\sigma)}$. The electrode is assumed to be in equilibrium, so that it can be characterized by the Fermi distribution $f(\omega) = \{1 + e^{\beta(\omega-\mu_0)}\}^{-1}$, with the inverse temperature $\beta = (k_B T)^{-1}$ and the chemical potential μ_0 set in the middle of spin-up and spin-down levels.

The last term in Eq. (2) stands for tunnel coupling between the single QD and side reservoir

$$V = \sum_\sigma (f_\sigma^\dagger d_\sigma + d_\sigma^\dagger f_\sigma), \tag{6}$$

where $f_\sigma \equiv \sum_k t_{k\sigma} c_{k\sigma}$, with $t_{k\sigma}$ the spin-dependent tunneling amplitude. The corresponding tunneling rate for an electron with spin σ is characterized by the intrinsic linewidth $\Gamma_\sigma(\omega) = 2\pi \sum_k |t_{k\sigma}|^2 \delta(\omega - \varepsilon_{k\sigma})$.

Hereafter, we assume wide band limit in the electrodes, which leads to energy independent tunneling rates $\Gamma_\sigma(\omega) = \Gamma_\sigma$. In what follows, we set the unit of $\hbar = e = 1$ for the Planck constant and electron charge, unless stated otherwise.

III. GQME AND SPIN DYNAMICS

The entire system (reduced system-plus-environment) is closed and its evolution is generated by the entire Hamiltonian in Eq. (2):

$$\rho_T(t) = U(t)\rho_T(0)U^\dagger(t), \tag{7a}$$

$$U(t) = \exp_+\left(-i\int_0^t d\tau H_T(\tau)\right), \tag{7b}$$

where $\rho_T(t)$ is the density matrix of the entire system at time t and $U(t)$ is the time-ordered evolution operator. In fact, we are not interested in tracking the dynamical evolution of the entire system. Instead, we would like to describe the reduced system by a dynamical equation that accounts for (usually approximately) the influence of the environment on the system state, while removing the need to track the full environment evolution. This is described by a reduced density matrix $\rho(t)$, which, in principle, can be obtained by tracing the density matrix of the entire system over the environment degrees of freedom, i.e., $\rho(t) = \mathrm{tr}_B[\rho_T(t)]$, where $\mathrm{tr}_B[\cdots]$ stands for the trace over the environment degrees of freedom.

In this work, we are not only interested in the dynamics of the reduced system but also energy and particle transport between the QD and side reservoir. One thus has to relate the reduced dynamics to the output of the system. The key quantity is the joint probability distribution $P(n_\uparrow, n_\downarrow, \varepsilon_\uparrow, \varepsilon_\downarrow, t)$, for observing an amount of spin-σ ($\sigma = \uparrow, \downarrow$) dependent particles n_σ and energy ε_σ flowing out of reservoir between time 0 and time t. The statistical properties of the energy and particle currents are completely characterized by the cumulant generating function (CGF) $\mathcal{F}(\boldsymbol{\chi}, t)$,

$$e^{\mathcal{F}(\boldsymbol{\chi},t)} = \sum_{n_\uparrow,n_\downarrow,\varepsilon_\uparrow,\varepsilon_\downarrow} P(n_\uparrow, n_\downarrow, \varepsilon_\uparrow, \varepsilon_\downarrow, t) \times e^{\mathrm{i}(n_\uparrow\chi_{1\uparrow}+n_\downarrow\chi_{1\downarrow}+\varepsilon_\uparrow\chi_{2\uparrow}+\varepsilon_\downarrow\chi_{2\downarrow})}, \tag{8}$$

where we have introduced $\boldsymbol{\chi} = \{\chi_{1\uparrow}, \chi_{1\downarrow}, \chi_{2\uparrow}, \chi_{2\downarrow}\}$, with $\chi_{1\sigma}$ the counting field related to the tunneling of spin σ electron and $\chi_{2\sigma}$ for energy transmission associated with σ spin. The statistics of particle and energy currents can be evaluated by simply taking derivatives of the CGF with corresponding counting fields.

It was shown that the relation between reduced dynamics and the output statistics is simply given by [22]

$$e^{\mathcal{F}(\boldsymbol{\chi},t)} = \mathrm{tr}[\rho_{\mathrm{T}}(\boldsymbol{\chi}, t)], \tag{9}$$

where $\mathrm{tr}[\cdots]$ denotes the trace over the degrees of freedom of the entire system (reduced system-plus-environment), and $\rho_{\mathrm{T}}(\boldsymbol{\chi}, t)$ is the $\boldsymbol{\chi}$-dependent density matrix of the entire system. Assuming that the counting starts at $t = 0$, then $\rho_{\mathrm{T}}(\boldsymbol{\chi}, 0) = \rho_{\mathrm{T}}(0)$, $\rho_{\mathrm{T}}(\boldsymbol{\chi}, t)$ satisfies [22,45,46]

$$\rho_{\mathrm{T}}(\boldsymbol{\chi}, t) = U(\boldsymbol{\chi}, t)\rho_{\mathrm{T}}(0)U^\dagger(-\boldsymbol{\chi}, t), \tag{10a}$$

$$U(\boldsymbol{\chi}, t) = \exp_+\left(-\mathrm{i}\int_0^t \mathrm{d}\tau H_{\mathrm{T}}(\boldsymbol{\chi}, \tau)\right). \tag{10b}$$

It is now clear that the evolution of $\rho_{\mathrm{T}}(\boldsymbol{\chi}, t)$ obeys a similar equation as $\rho_{\mathrm{T}}(t)$ in Eq. (7), with the only crucial difference that the entire Hamiltonian in Eq. (2) now becomes $\boldsymbol{\chi}$-dressed

$$H_{\mathrm{T}}(\boldsymbol{\chi}, t) = \exp\left\{\frac{\mathrm{i}}{2}\sum_\sigma\left(\chi_{1\sigma}N_{\mathrm{B}}^{(\sigma)} + \chi_{2\sigma}H_{\mathrm{B}}^{(\sigma)}\right)\right\}H_{\mathrm{T}}(t) \times \exp\left\{-\frac{\mathrm{i}}{2}\sum_\sigma\left(\chi_{1\sigma}N_{\mathrm{B}}^{(\sigma)} + \chi_{2\sigma}H_{\mathrm{B}}^{(\sigma)}\right)\right\}, \tag{11}$$

with $H_{\mathrm{B}}^{(\sigma)}$ and $N_{\mathrm{B}}^{(\sigma)}$ defined in Eqs. (4) and (5), respectively. Since the operators for the QD and reservoir commute, Eq. (11) can be readily expressed as

$$H_{\mathrm{T}}(\boldsymbol{\chi}, t) = H_{\mathrm{S}}(t) + H_{\mathrm{B}} + V(\boldsymbol{\chi}), \tag{12}$$

where $H_{\mathrm{S}}(t)$ and H_{B} remain unchanged. It is only the tunnel-coupling Hamiltonian that becomes counting fields dependent

$$V(\boldsymbol{\chi}) = \sum_\sigma\{f_\sigma(\boldsymbol{\chi})d_\sigma^\dagger + \mathrm{H.c.}\}, \tag{13}$$

with $f_\sigma(\boldsymbol{\chi}) = \sum_k t_{k\sigma}c_{k\sigma}e^{-\frac{\mathrm{i}}{2}(\chi_{1\sigma}+\chi_{2\sigma}\varepsilon_{k\sigma})}$.

If one were given $\rho_{\mathrm{T}}(\boldsymbol{\chi}, t)$ in Eq. (10), the $\boldsymbol{\chi}$-dependent reduced density matrix can be readily obtained via $\rho(\boldsymbol{\chi}, t) = \mathrm{tr}_{\mathrm{B}}\{\rho_{\mathrm{T}}(\boldsymbol{\chi}, t)\}$. The CGF in the steady state can be readily obtained as

$$\mathcal{F}(\boldsymbol{\chi}) = \lim_{t\to\infty}\frac{1}{t}\ln\{\mathrm{tr}_{\mathrm{S}}[\rho(\boldsymbol{\chi}, t)]\}, \tag{14}$$

where $\mathrm{tr}_{\mathrm{S}}[\cdots]$ means trace over the degrees of freedom of the reduced system. The central task thus is to obtain the GQME that the $\boldsymbol{\chi}$-dependent reduced density matrix $\rho(\boldsymbol{\chi}, t)$ satisfies.

Here, we assume that the system and reservoir are weakly coupled and perform a second-order perturbation expansion in terms of the coupling Hamiltonian. It is then followed by the conventional Born-Markov approximation but *without* invoking the widely used secular approximation [47]. To deal with the time-dependent system Hamiltonian, we work in the Floquet basis [48–51]. The GQME finally reads (a detailed derivation is referred to Appendix)

$$\dot{\rho}(\boldsymbol{\chi}, t) = -\mathrm{i}[H_{\mathrm{S}}(t), \rho(\boldsymbol{\chi}, t)] + \mathcal{R}(\boldsymbol{\chi})\rho(\boldsymbol{\chi}, t), \tag{15}$$

where the first term describes the free evolution. The second term stands for dissipation

$$\begin{aligned}
\mathcal{R}(\boldsymbol{\chi})\rho(\boldsymbol{\chi}, t) = &\left\{\Gamma_{0,+}(\boldsymbol{\chi})\mathcal{J}[|u_0(t)\rangle\langle u_+(t)|] - \frac{1}{2}\Gamma_{0,+}\mathcal{A}[|u_0(t)\rangle\langle u_+(t)|] - \frac{\mathrm{i}}{2}\kappa_{0,+}\mathcal{C}[|u_0(t)\rangle\langle u_+(t)|]\right\}\rho(\boldsymbol{\chi}, t)\\
&+\left\{\Gamma_{0,-}(\boldsymbol{\chi})\mathcal{J}[|u_0(t)\rangle\langle u_-(t)|] - \frac{1}{2}\Gamma_{0,-}\mathcal{A}[|u_0(t)\rangle\langle u_-(t)|] - \frac{\mathrm{i}}{2}\kappa_{0,-}\mathcal{C}[|u_0(t)\rangle\langle u_-(t)|]\right\}\rho(\boldsymbol{\chi}, t)\\
&+\left\{\Gamma_{+,0}(\boldsymbol{\chi})\mathcal{J}[|u_+(t)\rangle\langle u_0(t)|] - \frac{1}{2}\Gamma_{+,0}\mathcal{A}[|u_+(t)\rangle\langle u_0(t)|] - \frac{\mathrm{i}}{2}\kappa_{+,0}\mathcal{C}[|u_+(t)\rangle\langle u_0(t)|]\right\}\rho(\boldsymbol{\chi}, t)\\
&+\left\{\Gamma_{-,0}(\boldsymbol{\chi})\mathcal{J}[|u_-(t)\rangle\langle u_0(t)|] - \frac{1}{2}\Gamma_{-,0}\mathcal{A}[|u_-(t)\rangle\langle u_0(t)|] - \frac{\mathrm{i}}{2}\kappa_{-,0}\mathcal{C}[|u_-(t)\rangle\langle u_0(t)|]\right\}\rho(\boldsymbol{\chi}, t)\\
&-\{[\Upsilon_{0,-} + \mathrm{i}\xi_{0,-}]|u_+(t)\rangle\langle u_-(t)|\rho(\boldsymbol{\chi}, t) + [\Upsilon_{0,+} - \mathrm{i}\xi_{0,+}]\rho(\boldsymbol{\chi}, t)|u_+(t)\rangle\langle u_-(t)|\}\\
&-\{[\Upsilon_{0,+} + \mathrm{i}\xi_{0,+}]|u_-(t)\rangle\langle u_+(t)|\rho(\boldsymbol{\chi}, t) + [\Upsilon_{0,-} - \mathrm{i}\xi_{0,-}]\rho(\boldsymbol{\chi}, t)|u_-(t)\rangle\langle u_+(t)|\}\\
&+[\Upsilon_{+,0}(\boldsymbol{\chi}) + \mathrm{i}\xi_{+,0}(\boldsymbol{\chi}) + \Upsilon_{-,0}(\boldsymbol{\chi}) - \mathrm{i}\xi_{-,0}(\boldsymbol{\chi})]|u_+(t)\rangle\langle u_0(t)|\rho(\boldsymbol{\chi}, t)|u_0(t)\rangle\langle u_-(t)|\\
&+[\Upsilon_{0,+}(\boldsymbol{\chi}) - \mathrm{i}\xi_{0,+}(\boldsymbol{\chi}) + \Upsilon_{0,-}(\boldsymbol{\chi}) + \mathrm{i}\xi_{0,-}(\boldsymbol{\chi})]|u_0(t)\rangle\langle u_-(t)|\rho(\boldsymbol{\chi}, t)|u_+(t)\rangle\langle u_0(t)|\\
&+[\Upsilon_{+,0}(\boldsymbol{\chi}) - \mathrm{i}\xi_{+,0}(\boldsymbol{\chi}) + \Upsilon_{-,0}(\boldsymbol{\chi}) + \mathrm{i}\xi_{-,0}(\boldsymbol{\chi})]|u_-(t)\rangle\langle u_0(t)|\rho(\boldsymbol{\chi}, t)|u_0(t)\rangle\langle u_+(t)|\\
&+[\Upsilon_{0,+}(\boldsymbol{\chi}) + \mathrm{i}\xi_{0,+}(\boldsymbol{\chi}) + \Upsilon_{0,-}(\boldsymbol{\chi}) - \mathrm{i}\xi_{0,-}(\boldsymbol{\chi})]|u_0(t)\rangle\langle u_+(t)|\rho(\boldsymbol{\chi}, t)|u_-(t)\rangle\langle u_0(t)|,
\end{aligned} \tag{16}$$

which is expressed in the Floquet basis $|u_0(t)\rangle$, $|u_\pm(t)\rangle\rangle$ [see Eq. (A10)]. The involved superoperators are defined as $\mathcal{J}[r]\rho = r\rho r^\dagger$, $\mathcal{A}[r]\rho = r^\dagger r\rho + \rho r^\dagger r$, and $\mathcal{C}[r]\rho = [r^\dagger r, \rho]$. The first four lines describe the tunneling between QD and side reservoir in the Lindblad-like form, with $\Gamma_{0,\pm}$ the rate for an electron in Floquet state $|u_+(t)\rangle$ or $|u_-(t)\rangle$ to tunnel out of QD and $\Gamma_{\pm,0}$ for the opposite process. Their connections to the tunneling rates in the original reference $\Gamma_\sigma^{(\pm)}$ ($\sigma = \uparrow, \downarrow$) are given by Eqs. (A24) and (A25). The coefficients $\kappa_{0,\pm}$ and $\kappa_{\pm,0}$ arise purely from the energy renormalization [see Eq. (A26)].

The last six lines in Eq. (16) originate from the nonsecular treatment. This can be easily verified in Eq. (A23), where all these terms are oscillating in the interaction picture. In the case of fast oscillations, the effects of these terms will very quickly average to zero and can thus be neglected. Equation (16) then reduces to a Lindblad master equation, such that the populations and coherences of the density matrix are dynamically decoupled. In this work, we will go beyond the secular approximation and reveal its essential influence. The involved coefficients Υ and ξ, defined in Eqs. (A27) and (A28), are going to have important roles to play in an effective magnetic field, leading to prominent effects on the energy current.

Investigation of spin dynamics can be achieved by propagating Eq. (15) with $\chi = 0$. This can be done, for instance, in the Floquet basis with the diagonal density matrix elements $\rho_{00}(t) = \langle u_0(t)|\rho(t)|u_0(t)\rangle$, $\rho_{++}(t) = \langle u_+(t)|\rho(t)|u_+(t)\rangle$, and $\rho_{--}(t) = \langle u_-(t)|\rho(t)|u_-(t)\rangle$ describing populations, and off-diagonal density matrix elements $\rho_{+-}(t) = \langle u_+(t)|\rho(t)|u_-(t)\rangle$ and $\rho_{-+}(t) = \langle u_-(t)|\rho(t)|u_+(t)\rangle$ standing for coherences. Alternatively, in this work we reexpress them in terms of the probabilities and an average spin. We use ρ_{00} and $\rho_{11} = \rho_{++} + \rho_{--}$ to represent the probabilities to find an empty and occupied QD, respectively. We furthermore introduce the vector of average spin $\boldsymbol{S} = \{S_x, S_y, S_z\}$, where the individual components are given by

$$S_x = \frac{\rho_{+-} + \rho_{-+}}{2}, \quad S_y = \mathrm{i}\frac{\rho_{+-} - \rho_{-+}}{2}, \quad S_z = \frac{\rho_{++} - \rho_{--}}{2}. \tag{17}$$

Therefore, the dot state is characterized by $\rho(\boldsymbol{\chi}) = \{\rho_{00}, \rho_{11}, S_x, S_y, S_z\}$. According to GQME (15) and (16), it satisfies

$$\dot{\rho}(\boldsymbol{\chi}) = \mathcal{L}(\boldsymbol{\chi})\rho(\boldsymbol{\chi}, t), \tag{18}$$

where $\mathcal{L}(\boldsymbol{\chi})$ is a 5×5 matrix. Among these five equations, two are for the occupations probabilities and three are for the average spin. The first two read

$$\begin{aligned}\frac{\mathrm{d}}{\mathrm{d}t}\begin{pmatrix}\rho_{00}\\ \rho_{11}\end{pmatrix} =& \begin{pmatrix}-\Gamma_{+,0} - \Gamma_{-,0} & \frac{1}{2}\{\Gamma_{0,+}(\boldsymbol{\chi}) + \Gamma_{0,-}(\boldsymbol{\chi})\}\\ \Gamma_{+,0}(\boldsymbol{\chi}) + \Gamma_{-,0}(\boldsymbol{\chi}) & -\frac{1}{2}(\Gamma_{0,+} + \Gamma_{0,-})\end{pmatrix}\begin{pmatrix}\rho_{00}\\ \rho_{11}\end{pmatrix}\\ &+ 2\begin{pmatrix}\Upsilon_{0,+}(\boldsymbol{\chi}) + \Upsilon_{0,-}(\boldsymbol{\chi})\\ -\Upsilon_{0,+} - \Upsilon_{0,-}\end{pmatrix}S_x + 2\begin{pmatrix}\xi_{0,+}(\boldsymbol{\chi}) - \xi_{0,-}(\boldsymbol{\chi})\\ -\xi_{0,+} + \xi_{0,-}\end{pmatrix}S_y + \begin{pmatrix}\Gamma_{0,+}(\boldsymbol{\chi}) - \Gamma_{0,-}(\boldsymbol{\chi})\\ -\Gamma_{0,+} + \Gamma_{0,-}\end{pmatrix}S_z.\end{aligned} \tag{19}$$

Unambiguously, the occupation probabilities are coupled to the average spin in the QD, which is described by the remaining three equations

$$\frac{\mathrm{d}\boldsymbol{S}}{\mathrm{d}t} = \left(\frac{\mathrm{d}\boldsymbol{S}}{\mathrm{d}t}\right)_{\mathrm{acc}} + \left(\frac{\mathrm{d}\boldsymbol{S}}{\mathrm{d}t}\right)_{\mathrm{dec}} + \left(\frac{\mathrm{d}\boldsymbol{S}}{\mathrm{d}t}\right)_{\mathrm{pre}}. \tag{20}$$

The first term describes the spin accumulation due to tunneling between the electrode and QD

$$\left(\frac{\mathrm{d}\boldsymbol{S}}{\mathrm{d}t}\right)_{\mathrm{acc}} = \begin{pmatrix}\Upsilon_{-,0}(\boldsymbol{\chi}) + \Upsilon_{+,0}(\boldsymbol{\chi}), & -\frac{1}{2}(\Upsilon_{0,-} + \Upsilon_{0,+})\\ \xi_{-,0}(\boldsymbol{\chi}) - \xi_{+,0}(\boldsymbol{\chi}), & -\frac{1}{2}(\xi_{-,0} - \xi_{+,0})\\ \frac{1}{2}\{\Gamma_{+,0}(\boldsymbol{\chi}) - \Gamma_{-,0}(\boldsymbol{\chi})\}, & -\frac{1}{2}(\Gamma_{+,0} - \Gamma_{-,0})\end{pmatrix} \cdot \begin{pmatrix}\rho_{00}\\ \rho_{11}\end{pmatrix}. \tag{21}$$

This is the source term responsible for the building up of a spin polarization in the QD. The second term depicts the opposite mechanism—decay of the spin via tunneling out of spin

$$\left(\frac{\mathrm{d}\boldsymbol{S}}{\mathrm{d}t}\right)_{\mathrm{dec}} = -\frac{1}{2}(\Gamma_{0,+} + \Gamma_{0,-})\boldsymbol{S}. \tag{22}$$

Both spin accumulation and decay depend on the spin orientation, which is described by the third equation

$$\left(\frac{\mathrm{d}\boldsymbol{S}}{\mathrm{d}t}\right)_{\mathrm{pre}} = \boldsymbol{S} \times \boldsymbol{\mathcal{B}}. \tag{23}$$

Interestingly, this term describes the precession of the average spin about an effective magnetic field

$$\begin{aligned}\boldsymbol{\mathcal{B}} &= \{\mathcal{B}_x, \mathcal{B}_y, \mathcal{B}_z\}\\ &= \{-(\xi_{0,+} + \xi_{0,-}), (\Upsilon_{0,+} - \Upsilon_{0,-}), \tilde{\epsilon}\},\end{aligned} \tag{24}$$

with $\tilde{\epsilon} = \epsilon_- - \epsilon_+ + \frac{1}{2}(\kappa_{0,-} - \kappa_{0,+})$.

The x and y components of the effective magnetic field, i.e., $\mathcal{B}_x$ and $\mathcal{B}_y$, arise from the nonsecular treatment. In case the terms in the last six lines of Eq. (A23) experience fast oscillations, the effects of these terms will very rapidly average to zero. Then $\mathcal{B}_x$ and $\mathcal{B}_y$ have negligible contribution, and Eq. (16) reduces to the usual Born-Markov-Secular (BMS) master equation if $\boldsymbol{\chi} = 0$. The z component of the effective magnetic field $\mathcal{B}_z$ originates from the energy renormalization; see the last term in the first two lines of Eq. (16). Note that this effective magnetic field should not be confused with the real magnetic field $\boldsymbol{B}$ in Eq. (1). Without this real magnetic field $\boldsymbol{B}$, it will not have the Zeeman splitting of the single level, ESR, as well as the spin pumping process. In this case,

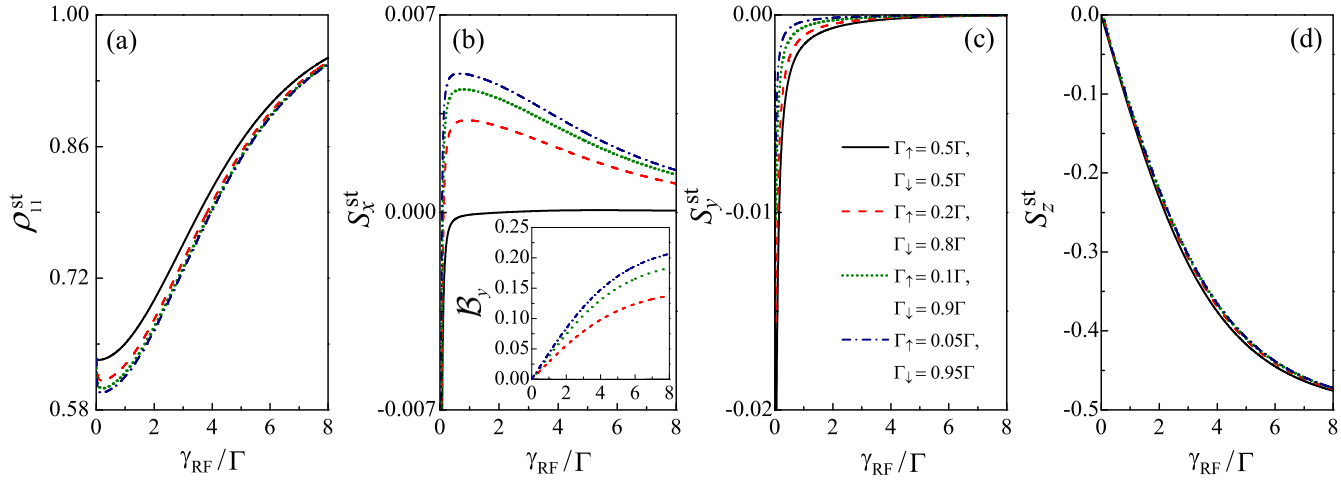

FIG. 2. Stationary occupation of the QD ($\rho_{11}^{\rm st}$) and accumulation of average spin ($S_x^{\rm st}$, $S_y^{\rm st}$, $S_z^{\rm st}$) in the basis of Floquet states versus Rabi frequency for different configurations of asymmetry in spin tunneling. We set $\Gamma = \Gamma_\uparrow + \Gamma_\downarrow$ as the reference of energy. Other plotting parameters are $\delta = 0$, $\Omega/\Gamma = 3.0$, $\beta\Gamma = 0.1$, and a wide bandwidth $w/\Gamma = 100$. The inset in Fig. 2(b) shows the y component of the effective magnetic field vs Rabi frequency.

the single level is in equilibrium with the bath, no net spin current flows, and thus spin accumulation in the quantum dot vanishes, $\boldsymbol{S} = 0$.

In the literature, effective magnetic fields (sometimes also called pseudomagnetic fields [52,53]) due to energy renormalization have been investigated, for example, in the singular coupling limit (SCL) [54–56]. Yet, the SCL normally implies a flat spectral density and high temperature limit $k_{\rm B}T \to \infty$, such that the system energy splitting can be hardly resolved. In this work, we employ the GQME with great importance in the following two aspects. First, the GQME is derived under the second order Born-Markov approximation and thus is valid as long as the temperature $k_{\rm B}T \gg \Gamma$. That means our GQME is valid in a wider temperature regime in comparison with the SCL. The preservation of positivity is guaranteed, which we have checked numerically throughout this work. Second, it is found from our GQME that the effective magnetic field originates not only from the energy renormalization (cf. $\mathcal{B}_z$), but also from the nonsecular treatment (see $\mathcal{B}_x$ and $\mathcal{B}_y$). Later, it will be demonstrated that, under the condition of strong asymmetry in spin tunneling, the components of the effective magnetic fields due to nonsecular treatment have even more important roles to play in energy flow through the system.

Figure 2 shows the stationary occupation of the QD ($\rho_{11}^{\rm st}$) and average spin accumulation $\{S_x^{\rm st}, S_y^{\rm st}, S_z^{\rm st}\}$ versus Rabi frequency for different configurations of asymmetry in spin tunneling. The probability of finding an empty QD ($\rho_{00}^{\rm st}$) is not displayed as it simply satisfies the probability conservation $\rho_{00}^{\rm st} + \rho_{11}^{\rm st} = 1$. The occupation of the QD ($\rho_{11}^{\rm st}$) first decreases, reaches a local minimum, and then grows rapidly towards unity with increasing Rabi frequency, cf. Fig. 2(a). In comparison, the results by using a BMS master equation [i.e., by neglecting the last six lines in Eq. (16)] is displayed in Fig. 3. The results using two approaches are consistent in the regime of large Rabi frequencies, as seen from the curves in Fig. 3. Yet, noticeable differences are observed for small $\gamma_{\rm RF}$, particularly in the case of a large asymmetry in spin tunneling.

The nonmonotonic behavior of $\rho_{11}^{\rm st}$ can be interpreted as follows. In the regime of small Rabi frequency, the terms in the last six lines of Eq. (A23) do not experience fast oscillations, therefore do not average to zero. It produces finite effective magnetic fields and causes the precession of the average spin. This increases the probability for an electron to tunnel out of the QD, resulting thus in a reduction of the occupation $\rho_{11}^{\rm st}$. As $\gamma_{\rm RF}$ increases, the spin flipping process dominates. The electron is thus inclined to stay in the QD, leading to the increase of $\rho_{11}^{\rm st}$ with rising Rabi frequency. This explains the nonmonotonic behavior of the $\rho_{11}^{\rm st}$. Our results also show unambiguously that it is not justified to use the secular approximation in the regime of small Rabi frequencies.

In the limit of large Rabi frequency, an electron tunneled into the QD will be almost localized in the Floquet state "$|u_-(t)\rangle$" as indicated in $S_z^{\rm st}$, cf. Fig. 2(d). The y component of the average spin decays fast to zero, regardless of the asymmetry in spin tunneling, as shown in Fig. 2(c). It seems

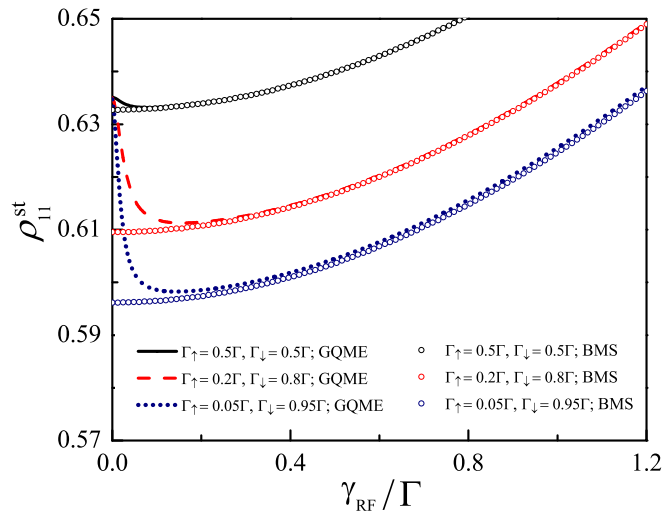

FIG. 3. Comparison of stationary occupation in QD ($\rho_{11}^{\rm st}$) using GQME (curves) and BMS master equation (symbols) in the basis of the Floquet states for various asymmetries in spin tunneling. All other plotting parameters are the same as those in Fig. 2.

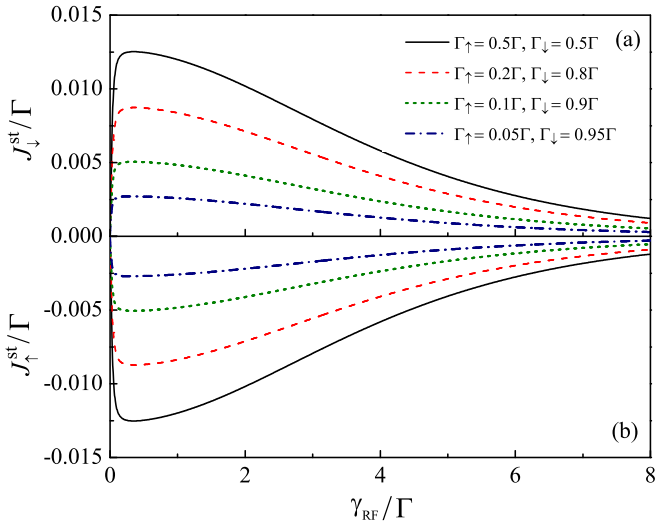

FIG. 4. Individual stationary spin currents $J_\downarrow^{st}$ and $J_\uparrow^{st}$ vs Rabi frequency for various configurations of spin tunneling asymmetry. All other plotting parameters are the same as those in Fig. 2.

to be consistent with the usual secular treatment. However, the x component of the average spin may survive for a wide range of Rabi frequency, depending on asymmetry in spin tunneling, see Fig. 2(b). We therefore emphasize that the use of a simple BMS master equation may overlook some important dynamics of the reduced system. We will further reveal later that the finite spin accumulation in the QD would have a significant influence on the energy flow through the system.

In the long time limit, Eq. (14) reduces to

$$\mathcal{F}(\boldsymbol{\chi}) = z_0(\boldsymbol{\chi}), \tag{25}$$

where $z_0(\boldsymbol{\chi})$ is the dominant eigenvalue with smallest magnitude of $\mathcal{L}(\boldsymbol{\chi})$ defined in Eq. (18) and satisfies $z_0(\boldsymbol{\chi}\to\mathbf{0}) = 0$ [57]. The individual stationary spin-σ current can be simply obtained as

$$J_\sigma^{st} = (-\mathrm{i})\frac{\partial}{\partial\chi_{1\sigma}} z_0(\boldsymbol{\chi})|_{\boldsymbol{\chi}\to 0}. \tag{26}$$

Throughout this work, the superscript "st" is used to represent stationary values. One straightforwardly gets the stationary spin up and spin down currents, respectively, as

$$\begin{aligned} J_\uparrow^{st} = {} & \tfrac{1}{2}(\Gamma_{0,+}^{(\uparrow)} + \Gamma_{0,-}^{(\uparrow)})\rho_{11}^{st} - [\Gamma_{+,0}^{(\uparrow)} + \Gamma_{-,0}^{(\uparrow)}]\rho_{00}^{st} \\ & - 2[\Upsilon_{0,+}^{(\uparrow)} + \Upsilon_{0,-}^{(\uparrow)}]S_x^{st} - 2[\xi_{0,+}^{(\uparrow)} - \xi_{0,-}^{(\uparrow)}]S_y^{st} \\ & + (\Gamma_{0,+}^{(\uparrow)} - \Gamma_{0,-}^{(\uparrow)})S_z^{st}, \end{aligned} \tag{27a}$$

$$\begin{aligned} J_\downarrow^{st} = {} & \tfrac{1}{2}(\Gamma_{0,+}^{(\downarrow)} + \Gamma_{0,-}^{(\downarrow)})\rho_{11}^{st} - [\Gamma_{+,0}^{(\downarrow)} + \Gamma_{-,0}^{(\downarrow)}]\rho_{00}^{st} \\ & + 2[\Upsilon_{0,+}^{(\downarrow)} + \Upsilon_{0,-}^{(\downarrow)}]S_x^{st} + 2[\xi_{0,+}^{(\downarrow)} - \xi_{0,-}^{(\downarrow)}]S_y^{st} \\ & + (\Gamma_{0,+}^{(\downarrow)} - \Gamma_{0,-}^{(\downarrow)})S_z^{st}, \end{aligned} \tag{27b}$$

where ρ_{jj}^{st} $(j = 0, 1)$ and S_ζ^{st} $(\zeta = x, y, z)$ are, respectively, the stationary solutions of Eqs. (19) and (20) in the limit $\boldsymbol{\chi}\to 0$.

Figure 4 shows the individual spin currents versus Rabi frequency for various configurations of spin tunneling asymmetry. The spin down current $(J_\downarrow^{st})$ is positive as it flows out of the QD, while the spin up current $(J_\uparrow^{st})$ is negative as it goes into the QD. Whenever an electron tunnels into QD, it will flow out of it. The stationary charge current is thus zero due to charge conservation:

$$J_{ch}^{st} = J_\uparrow^{st} + J_\downarrow^{st} = 0. \tag{28}$$

This is also confirmed by using Eq. (19). It is worthwhile to mention that this result holds regardless of the degree of asymmetry in spin tunneling.

As the Rabi frequency increases, the ESR and spin flipping process start to take place. This opens the possibility for a spin up electron tunnel into QD and a spin down electron tunnel out of the QD. The magnitude of either spin-up or spin-down current thus increases rapidly with Rabi frequency. In the opposite regime of large Rabi frequency, both fall off gradually towards zero with rising γ_{RF}. It is due to the fact that the electron is inclined to stay in the Floquet state "$|u_-(t)\rangle$" as the Rabi frequency increases, cf. Fig. 2(b). A so-called dynamical spin blockade mechanism develops [58–62], which leads eventually to a strong suppression of the spin currents. This explains the nonmonotonic behavior as shown in Fig. 4. Furthermore, the dynamical spin blockade is more pronounced for a large asymmetry in spin tunneling. That is the reason that an increase in spin tunneling asymmetry results in an overall inhibition of both spin-up and spin-down currents, see Fig. 4.

With the knowledge of individual spin up and spin down currents, we define the net spin current in close connection to real experiments [63,64], where a pure spin current is generated without an accompanying charge current by pushing spin-up electrons to move in one direction and an equal number of spin-down electrons to move in the opposite direction. Thereby the net charge current vanishes in the stationary limit $J_{ch} = J_\uparrow^{st} + J_\downarrow^{st} = 0$, see also Eq. (28). Yet, the net spin current defined as

$$J_{sp}^{st} \equiv J_\uparrow^{st} - J_\downarrow^{st} = 2J_\uparrow^{st} \tag{29}$$

is nonzero. Here we have used the charge conservation, i.e., Eq. (28).

The stationary energy currents, associated with the spin up and spin down currents, can be obtained in an analogous way

$$I_\sigma^{st} = (-\mathrm{i})\frac{\partial}{\partial\chi_{2\sigma}} z_0(\boldsymbol{\chi})|_{\boldsymbol{\chi}\to 0}. \tag{30}$$

By utilizing Eq. (18), one immediately arrives at

$$\begin{aligned} I_\uparrow^{st} = {} & \big(\epsilon_+ - \epsilon_0 - \tfrac{\Omega}{2}\big)\big\{\Gamma_{0,+}^{(\uparrow)}\rho_{++}^{st} - \Gamma_{+,0}^{(\uparrow)}\rho_{00}^{st} \\ & - 2\Upsilon_{0,+}^{(\uparrow)}S_x^{st} - 2\xi_{0,+}^{(\uparrow)}S_y^{st}\big\} \\ & + \big(\epsilon_- - \epsilon_0 - \tfrac{\Omega}{2}\big)\big\{\Gamma_{0,-}^{(\uparrow)}\rho_{--}^{st} - \Gamma_{-,0}^{(\uparrow)}\rho_{00}^{st} \\ & - 2\Upsilon_{0,-}^{(\uparrow)}S_x^{st} + 2\xi_{0,-}^{(\uparrow)}S_y^{st}\big\}, \end{aligned} \tag{31a}$$

$$\begin{aligned} I_\downarrow^{st} = {} & \big(\epsilon_+ - \epsilon_0 + \tfrac{\Omega}{2}\big)\big\{\Gamma_{0,+}^{(\downarrow)}\rho_{++}^{st} - \Gamma_{+,0}^{(\downarrow)}\rho_{00}^{st} \\ & + 2\Upsilon_{0,+}^{(\downarrow)}S_x^{st} + 2\xi_{0,+}^{(\downarrow)}S_y^{st}\big\} \\ & + \big(\epsilon_- - \epsilon_0 + \tfrac{\Omega}{2}\big)\big\{\Gamma_{0,-}^{(\downarrow)}\rho_{--}^{st} - \Gamma_{-,0}^{(\downarrow)}\rho_{00}^{st} \\ & + 2\Upsilon_{0,-}^{(\downarrow)}S_x^{st} - 2\xi_{0,-}^{(\downarrow)}S_y^{st}\big\}. \end{aligned} \tag{31b}$$

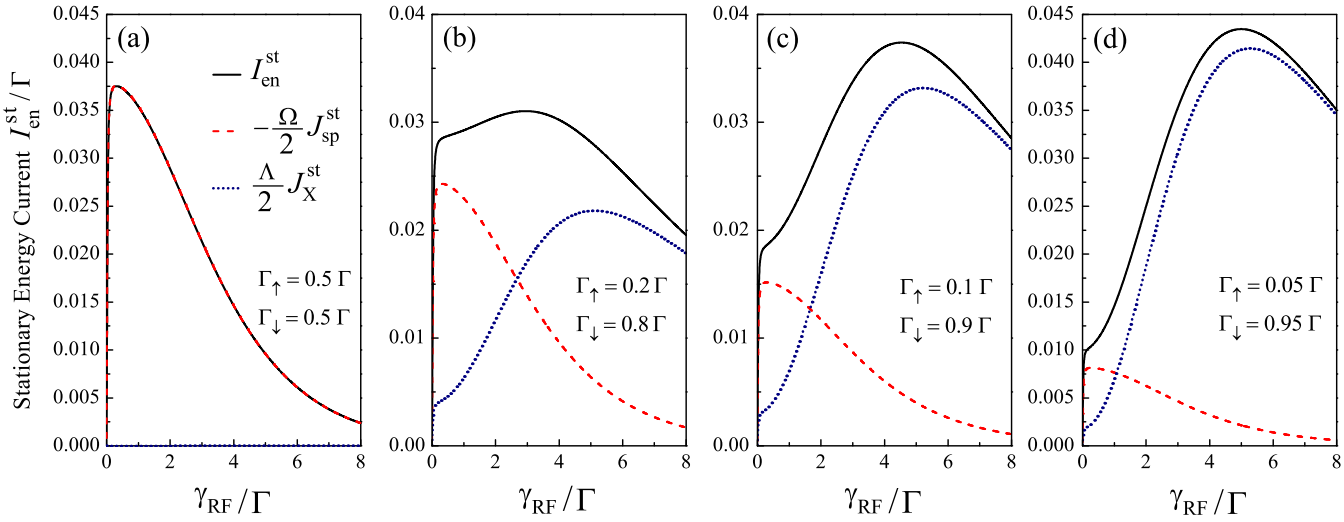

FIG. 5. Stationary energy current vs Rabi frequency for different configurations of spin tunneling asymmetry. For comparison, the contributions from spin current ($-\frac{\Omega}{2}J^{st}_{sp}$) and spin-magnetic field interaction ($\frac{\Lambda}{2}J^{st}_{X}$) are also shown in dashed and dotted curves, respectively. All other plotting parameters are the same as those in Fig. 2.

The total energy current in the steady state is the sum of individual energy currents and can be readily obtained as

$$I^{st}_{en} = I^{st}_{\uparrow} + I^{st}_{\downarrow} = -\frac{\Omega}{2}J^{st}_{sp} + \frac{\Lambda}{2}J^{st}_{X}, \tag{32}$$

where $\Lambda = \sqrt{\delta^2 + 4\gamma_{rf}^2}$ [see also Eqs. (A10) and (A11) in Appendix]. Unambiguously, it is made up of two components. The first contribution comes from the pure spin current J^{st}_{sp}. The second term originates from the interaction between the accumulated spin and the effective magnetic field

$$J^{st}_{X} = 4\big(S^{st}_{x}\mathcal{B}_y - S^{st}_{y}\mathcal{B}_x\big), \tag{33}$$

where $\mathcal{B}_x$ and $\mathcal{B}_y$ are, respectively, the x and y components of the effective magnetic field in Eq. (24). We emphasize that the result in Eq. (32) is of great significance in the following two aspects. First, an energy current can be produced even in the absence of a net matter (charge) current. This is independent of whether the secular approximation is made or not. Second, the interaction between the effective magnetic field and accumulated spin is also responsible for the production of an energy current. This contribution purely originates from the nonsecular treatment. It will be revealed that this term has essential roles to play in the energy flow under the circumstance of strongly asymmetric spin tunneling rates.

In Fig. 5 the stationary energy current (I^{st}_{en}) is plotted against Rabi frequency (γ_{RF}) for various configurations of spin tunneling asymmetry. The contributions due to spin current and spin accumulation are also exhibited by the dashed and dotted curves, respectively. In the case of symmetric spin tunneling ($\Gamma_\uparrow = \Gamma_\downarrow = 0.5\Gamma$), the spin accumulation (J^{st}_{X}) has a negligible contribution and the energy current is dominated by the spin current (J^{st}_{sp}), cf. Fig. 5(a). The behavior of the total energy current is thus similar to the spin current in Fig. 4, i.e., it first increases rapidly with rising Rabi frequency, reaches a maximum at approximately $\gamma_{RF} \approx 0.5\Gamma$, and finally falls off and approaches zero in the limit $\gamma_{RF} \to \infty$.

The picture becomes drastically different under the circumstance of strong asymmetry in spin tunneling, where the spin current is suppressed while the contribution from interaction between effective magnetic field and spin accumulation has an essential role to play. For instance, a strong asymmetry of $\Gamma_\uparrow = 0.2\Gamma$ and $\Gamma_\downarrow = 0.8\Gamma$ gives rise to a prominent enhancement in $\frac{\Lambda}{2}J^{st}_{X}$ at approximately $\gamma_{RF} \approx 5\Gamma$. This is ascribed to noticeable effective magnetic field $\mathcal{B}_y$ [inset of Fig. 2(b)] and finite spin accumulation S^{st}_{x} [Fig. 2(b)] [S^{st}_{y} has a vanishing contribution, cf. Fig. 2(c)]. It leads to the emergence of a local maximum in the energy current at $\gamma_{RF} \approx 3\Gamma$, in addition to its original maximum at $\gamma_{RF} \approx 0.5\Gamma$, see Fig. 5(b). Remarkably, for an extremely asymmetric tunneling rates ($\Gamma_\uparrow = 0.05\Gamma$, $\Gamma_\downarrow = 0.95\Gamma$) as shown in Fig. 5(d), the J^{st}_{X} term serves as the dominant contribution. As a result, one observes solely a single maximum in energy current at $\gamma_{RF} \approx 5\Gamma$. Our results show unambiguously the importance of considering the interaction between effective magnetic field and spin accumulation for very asymmetric spin tunneling rates. In this case, the use of a simple BMS master equation picture would be fundamentally insufficient.

IV. STOCHASTIC THERMODYNAMICS

Now we are in a position to discuss the stochastic thermodynamics, i.e., the identification of the first and second laws at the microscopic level. Our analysis is based on the two-measurement process theory and the method of counting statistics [22]. We will focus on energy and entropy balance of the ESR pumped QD system in the steady-state limit.

A. Energy balance based on statistics of work and heat

In this subsection we characterize the steady fluctuations of work and heat by evaluating their counting statistics using initial and final measurements of the system energy. Statistics of work has previously been analyzed with quantum jump approach [65] or Lindblad quantum master equations [66]. Here

we employ the two-measurement process approach [22,67] within the framework of the GQME, thus fully accounting for effect of the nonsecular treatment and the coherences.

Let us denote the instantaneous eigenenergies of $H_S(t)$ as $e_m(t)$ and those of H_B as ε_k. Assume that at time $t=0$ a joint measurement of $H_S(0)$ and H_B is performed, yielding the outcomes $e_m(0)$ and ε_k, respectively. At time $t>0$, a second joint measurement of $H_S(t)$ and H_B is made with outcomes $e_n(t)$ and $\varepsilon_{k'}$. The energy changes of system and bath, Δe and $\Delta\varepsilon$, respectively, in a single realization of the protocol are thus given by

$$\Delta e = e_n(t) - e_m(0), \tag{34a}$$

$$\Delta\varepsilon = \varepsilon_{k'} - \varepsilon_k. \tag{34b}$$

The change of the internal energy of the entire system is given by the sum of the energy changes of the reduced system and bath energies, apart from a negligible contribution due to the system-bath interaction. On the other hand, the entire system as a whole is isolated, with the exception of the driving protocol, which performs work on the open system. Since no heat enters the isolated entire system, the change of internal energy of the entire system is only due to the energy conveyed to the system by this driving protocol, which simply means that

$$W = \Delta e + \Delta\varepsilon = e_n(t) + \varepsilon_{k'} - e_m(0) - \varepsilon_k. \tag{35}$$

Apparently, W is a random variable due to the intrinsic randomness in the quantum measurement processes. The statistical properties of W can be conveniently expressed in terms of its characteristic function

$$G_W(\chi_W,t) = \int_{-\infty}^{\infty} \mathrm{d}W e^{\mathrm{i}W\chi_W} P(W,t), \tag{36}$$

where $P(W,t)$ is probability density function of observing an amount of work W performed by the external driving from time 0 to t, and χ_W is the corresponding counting field. According to the theory of two-measurement process [22], the probability density function is given by

$$P(W,t) = \sum_{e_n(t),e_m(0)} \sum_{\varepsilon_k,\varepsilon_{k'}} \delta[e_n(t)+\varepsilon_{k'} - e_m(0) - \varepsilon_k - W] \times p(e_n(t)+\varepsilon_{k'}|e_m(0)+\varepsilon_k) p(e_m(0)+\varepsilon_k), \tag{37}$$

where $p(e_n(t)+\varepsilon_{k'}|e_m(0)+\varepsilon_k)$ is the conditional probability that a measurement of $H_S(t)$ and H_B gives $e_n(t)$ and $\varepsilon_{k'}$, respectively, at time t given that it gave $e_m(0)$ and ε_k at time 0, while $p(e_m(0)+\varepsilon_k)$ is the usual probability to have $e_m(0)$ and ε_k at time 0.

By introducing the projectors $\hat{\mathcal{P}}_{e_j(t)}$ and $\hat{\mathcal{P}}_{\varepsilon_k}$ on the jth state of the system with energy $e_j(t)$ and kth state of the reservoir with energy ε_k, one has

$$p(e_n(t)+\varepsilon_{k'}|e_m(0)+\varepsilon_k)p(e_m(0)+\varepsilon_k) = \mathrm{tr}\big[\hat{\mathcal{P}}_{e_n(t)}\hat{\mathcal{P}}_{\varepsilon_{k'}} U(t) \hat{\mathcal{P}}_{e_m(0)}\hat{\mathcal{P}}_{\varepsilon_k}\rho_T(0) \times \hat{\mathcal{P}}_{\varepsilon_k}\hat{\mathcal{P}}_{e_m(0)}U^\dagger(t)\hat{\mathcal{P}}_{\varepsilon_{k'}}\hat{\mathcal{P}}_{e_n(t)}\big], \tag{38}$$

where $\mathrm{tr}[\cdots]$ represents the trace over the degrees of the freedom of the entire system and $U(t)$ is given by Eq. (7). Next we assume that the initial total density matrix can be factorized to $\rho_T(0) = \frac{e^{-\beta H_S(0)}}{Z_S(0)} \otimes \frac{e^{-\beta H_B}}{Z_B}$, where $Z_S(0) = \mathrm{tr}_S\{e^{-\beta H_S(0)}\}$ is the partition function of system at time $t=0$ and $Z_B = \mathrm{tr}_B\{e^{-\beta H_B}\}$ is that of the reservoir. By using $\hat{\mathcal{P}}^2_{e_j(t)} = \hat{\mathcal{P}}_{e_j(t)}$ and $\hat{\mathcal{P}}^2_{\varepsilon_k} = \hat{\mathcal{P}}_{\varepsilon_k}$, Eq. (38) is further simplified to

$$p(e_n(t)+\varepsilon_{k'}|e_m(0)+\varepsilon_k)p(e_m(0)+\varepsilon_k) = \mathrm{tr}\big[U^\dagger(t)\hat{\mathcal{P}}_{e_n(t)}\hat{\mathcal{P}}_{\varepsilon_{k'}}U(t)\hat{\mathcal{P}}_{e_m(0)}\hat{\mathcal{P}}_{\varepsilon_k}\rho_T(0)\big]. \tag{39}$$

Noticing that $\sum_{e_j(t)} \hat{\mathcal{P}}_{e_j(t)} e^{\pm\mathrm{i}\chi_W e_j(t)} = e^{\pm\mathrm{i}\chi_W H_S(t)}$ and $\sum_{\varepsilon_k} \hat{\mathcal{P}}_{\varepsilon_k} e^{\pm\mathrm{i}\chi_W\varepsilon_k} = e^{\pm\mathrm{i}\chi_W H_B}$, the characteristic function of work in Eq. (36) can be written as

$$\begin{aligned} G_W(\chi_W,t) &= \mathrm{tr}\Big\{e^{\mathrm{i}\frac{\chi_W}{2}[H_S(t)+H_B]}U(t)e^{-\mathrm{i}\frac{\chi_W}{2}[H_S(0)+H_B]}\rho_T(0) \\ &\quad\times e^{-\mathrm{i}\frac{\chi_W}{2}[H_S(0)+H_B]}U^\dagger(t)e^{\mathrm{i}\frac{\chi_W}{2}[H_S(t)+H_B]}\Big\}, \\ &= \sum_{e_n(t),e_m(0)} \frac{e^{\mathrm{i}\chi_W[e_n(t)-e_m(0)]-\beta e_m(0)}}{Z_S(0)} \\ &\quad\times \langle e_n(t)|\varrho(\chi_W,t;e_m(0))|e_n(t)\rangle, \end{aligned} \tag{40}$$

where we have introduced a new density matrix of the reduced system including the counting field of work

$$\varrho(\chi_W,t;e_m(0)) = \mathrm{tr}_B\Big\{e^{\mathrm{i}\frac{\chi_W}{2}H_B}U(t)e^{-\mathrm{i}\frac{\chi_W}{2}H_B}\varrho(0;e_m(0)) \otimes \rho_B\, e^{-\mathrm{i}\frac{\chi_W}{2}H_B}U^\dagger(t)e^{\mathrm{i}\frac{\chi_W}{2}H_B}\Big\}, \tag{41}$$

with the initial condition $\varrho(0;e_m(0)) = |e_m(0)\rangle\langle e_m(0)|$. By comparing with Eqs. (10) and (11), one finds that $\varrho(\chi_W,t;e_m(0))$ satisfies the same equation as $\rho(\boldsymbol{\chi},t)$ does, i.e., Eq. (18), with only the crucial replacement

$$\varrho(\chi_W,t;e_m(0)) = \rho(\boldsymbol{\chi},t)|_{\chi_{1\uparrow}=\chi_{1\downarrow}=0,\chi_{2\uparrow}=\chi_{2\downarrow}=\chi_W}. \tag{42}$$

It is thus expected both populations and coherences have important roles to play in the statistics of work. Here, we are interested in the stationary statistics, therefore, the CGF of the mechanical power is simply given by

$$\begin{aligned} \mathcal{G}_W(\chi_W,t) &= \lim_{t\to\infty}\frac{1}{t}\ln G_W(\chi_W,t) \\ &= z_0(\boldsymbol{\chi})|_{\chi_{1\uparrow}=\chi_{1\downarrow}=0,\chi_{2\uparrow}=\chi_{2\downarrow}=\chi_W}, \end{aligned} \tag{43}$$

where $z_0(\boldsymbol{\chi})$ is the dominant eigenvalue with the smallest magnitude of $\mathcal{L}(\boldsymbol{\chi})$ as shown in Eq. (25).

The average rate of mechanical work is simply obtained

$$\begin{aligned} \dot{W} &= -\mathrm{i}\frac{\partial}{\partial\chi_W} z_0(\{0,0,\chi_W,\chi_W\})|_{\chi_W\to 0} \\ &= I^{\mathrm{st}}_\uparrow + I^{\mathrm{st}}_\downarrow = -\frac{\Omega}{2}J^{\mathrm{st}}_{\mathrm{sp}} + \frac{\Lambda}{2}J^{\mathrm{st}}_X. \end{aligned} \tag{44}$$

It shows clearly that the work done on the system is used to produce a spin current and a precession of an average spin in the QD, where the latter originates purely from nonsecular treatment.

In comparison with the conventional results where the work done onto a system contains a contribution due to a matter current, we provide an essential system that work is not associated with a net charge current but a pure spin current through the system. Furthermore, we reveal that it is the work done onto the system that leads essentially to a

subtle interaction between an average spin and an effective magnetic field, generating thus the precession of the average spin about the effective field. We further remind the following two observations. First, the driving is important, otherwise the single level is in equilibrium with the bath and spin accumulation in the quantum dot is zero. Second, the nonsecular treatment is also essential to this interaction. Under the secular approximation, only the z component of the effective magnetic $\mathcal{B}_z$ may survive, which, however, does not have any contribution to the energy current, cf. Eq. (33). Our work thus demonstrates the importance of the nonsecular treatment in similar systems.

The statistical properties of the heat flow can be analyzed in a similar way by using the two-measurement process theory [22,68]. Assume at time $t = 0$ a measurement $H_{\rm B}$ yields an outcome ε_k. A little later at $t > 0$, a second measurement is made with outcome $\varepsilon_{k'}$. The heat flow from the reservoir to the QD is given by

$$Q = -(\varepsilon_{k'} - \varepsilon_k). \tag{45}$$

Analogously to Eq. (36), the characteristic function of heat flow is defined as

$$G_Q(\chi_Q, t) = \int_{-\infty}^{\infty} {\rm d}Q e^{{\rm i}Q\chi_Q} P(Q, t), \tag{46}$$

where χ_Q is the counting field associated with heat flow, and $P(Q, t)$ is the probability density function of observing an amount of heat Q flowed in to QD from time 0 to t. It can be determined from the two-time measurement approach [22]:

$$P(Q, t) = \sum_{\varepsilon_k, \varepsilon_{k'}} \delta[\varepsilon_{k'} - \varepsilon_k + Q)] p(\varepsilon_{k'}|\varepsilon_k) p(\varepsilon_k), \tag{47}$$

where $p(\varepsilon_{k'}|\varepsilon_k)$ is the conditional probability for observing $\varepsilon_{k'}$ at time t, given that it yields ε_k at time 0, while $p(\varepsilon_k)$ is the usual probability to have ε_k at time 0. By following similar procedures in Eqs. (38) and (39), the characteristic function of heat flow can be expressed as

$$G_Q(\chi_Q, t) = {\rm tr}_{\rm S}[\varrho(-\chi_Q, t)], \tag{48}$$

where $\varrho(-\chi_Q, t)$ satisfies the same equation as $\rho(\boldsymbol{\chi}, t)$ in Eq. (18), with only the replacement $\varrho(-\chi_Q, t) = \rho(\boldsymbol{\chi}, t)|_{\chi_{1\uparrow}=\chi_{1\downarrow}=0, \chi_{2\uparrow}=\chi_{2\downarrow}=-\chi_Q}$. In comparison with Eq. (25), one immediately finds the CGF of the heat flow in the stationary limit

$$\begin{aligned} \mathcal{G}_Q(\chi_Q) &= \lim_{t\to\infty} \frac{1}{t} \ln G_Q(\chi_Q, t) \\ &= z_0(\boldsymbol{\chi})_{\chi_{1\uparrow}=\chi_{1\downarrow}=0, \chi_{2\uparrow}=\chi_{2\downarrow}=-\chi_Q}, \end{aligned} \tag{49}$$

where $z_0(\boldsymbol{\chi})$ is the dominant eigenvalue with the smallest magnitude of $\mathcal{L}(\boldsymbol{\chi})$ in Eq. (25). The average heat flowing into QD is simply given by

$$\begin{aligned} \dot{Q} &= -{\rm i}\frac{\partial}{\partial \chi_Q} z_0(\{0, 0, -\chi_Q, -\chi_Q\})|_{\chi_Q\to 0} \\ &= -(I^{\rm st}_{\uparrow} + I^{\rm st}_{\downarrow}). \end{aligned} \tag{50}$$

By comparing with Eqs. (44), one eventually arrives at the energy balance relation in terms of the first law of thermodynamics

$$\dot{E} = \dot{Q} + \dot{W} = 0. \tag{51}$$

The work done on the system is completely converted into heat, such that the net increase of energy in the QD is zero in the stationary limit.

B. Entropy balance

We start with the von Neumann entropy

$$S(t) = -{\rm tr}_{\rm S}[\rho(t) \ln \rho(t)], \tag{52}$$

where $\rho(t)$ is the density matrix of the reduced system. The change in von Neumann entropy ΔS can be decomposed into an entropy production $\Delta S_{\rm i}$ and an entropy flow $\Delta S_{\rm e}$ [69–72], where the latter is given by the heat exchanged with the reservoir multiplied by the inverse temperature

$$\Delta S_{\rm e} = \beta \Delta Q. \tag{53}$$

The rate of change of the entropy production then is given by

$$\dot{S}_{\rm i} = \dot{S} - \beta \dot{Q}, \tag{54}$$

where $\dot{S} = -{\rm tr}_{\rm S}[\dot{\rho}(t) \ln \rho(t)]$ due to ${\rm tr}_{\rm S}[\dot{\rho}(t)] = 0$. On the other hand, the internal energy of the reduced system is given by $E = {\rm tr}_{\rm S}[H_{\rm S}(t)\rho(t)]$. Its rate of change can be decomposed into the contribution from work $\dot{W} = {\rm tr}_{\rm S}[\dot{H}_{\rm S}(t)\rho(t)]$ and that from heat flow $\dot{Q} = {\rm tr}_{\rm S}[H_{\rm S}(t)\dot{\rho}(t)]$, verifying thus the the first law of thermodynamics $\dot{E} = \dot{Q} + \dot{W}$. The entropy production in Eq. (54) can be reexpressed as

$$\dot{S}_{\rm i} = -{\rm tr}_{\rm S}\{\dot{\rho}(t)[\ln \rho(t) - \ln \rho_{\rm G}(t)]\}, \tag{55}$$

where we have defined an instantaneous density matrix representing an ideal Gibbs' state at time t

$$\rho_{\rm G}(t) = \frac{e^{-\beta H_{\rm S}(t)}}{Z_{\rm G}(t)}, \tag{56}$$

with $Z_{\rm G}(t) = {\rm tr}_{\rm S}[e^{-\beta H_{\rm S}(t)}]$. According to Eq. (18), the entropy production can also be rewritten as

$$\dot{S}_{\rm i} = -{\rm tr}_{\rm S}\{\mathcal{L}(\boldsymbol{\chi} = 0)\rho(t)[\ln \rho(t) - \ln \rho_{\rm G}(t)]\}. \tag{57}$$

In the stationary limit, the rate of entropy change in the system vanishes, i.e., $\dot{S} = 0$, so that

$$\dot{S}_{\rm i} = -\dot{S}_{\rm e} = -\beta \dot{Q} = \beta I^{\rm st}_{\rm en} \geqslant 0. \tag{58}$$

Our analysis thus shows the validity of Eq. (58) beyond a Lindblad description.

In Fig. 6, the entropy production rate is plotted for different configurations of spin tunneling asymmetry. For a small Rabi frequency $\gamma_{\rm RF}/\Gamma = 0.5$, the entropy production rate falls off rapidly to the stationary value given by Eq. (58), see Fig. 6(a). As the symmetry of spin tunneling increases, the stationary value decreases, consistent with the energy current in Fig. 5. In the case of a large Rabi frequency ($\gamma_{\rm RF}/\Gamma = 5.0$), the entropy production rate undergoes fast oscillations before it reaches its steady state, as shown in Fig. 6(b). Its stationary value, however, grows as the symmetry of spin tunneling enhances. This is also consistent with the energy current for a large Rabi frequency. For a wide valid parameter regime, we do not observe negative entropy production. Our results thus shows numerically the second law to be respected.

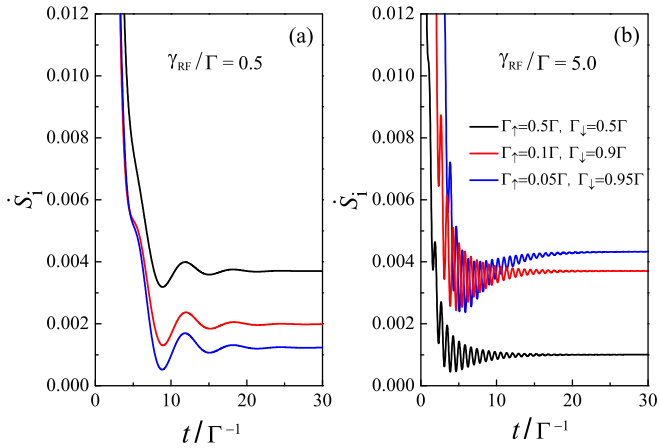

FIG. 6. Entropy production rate for different configurations of spin tunneling asymmetry with (a) $\gamma_{RF}/\Gamma = 0.5$ and (b) $\gamma_{RF}/\Gamma = 5.0$. All other plotting parameters are the same as those in Fig. 2.

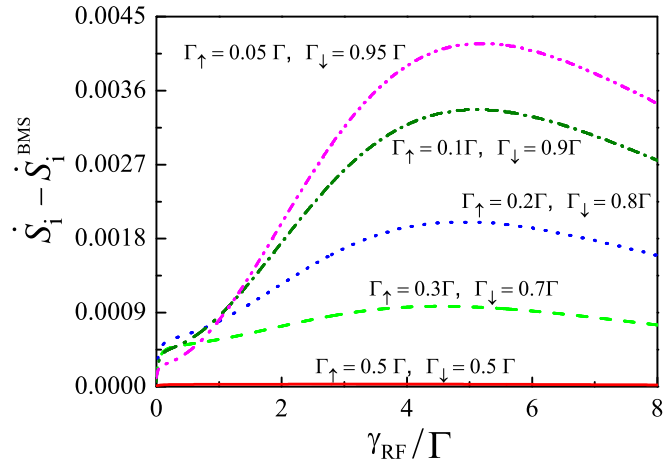

FIG. 7. The difference between the stationary entropy production rate evaluated by our GQME approach $\dot{S}_i$ and that by BMS master equation $\dot{S}_i^{BMS}$, versus Rabi frequency for different configurations of spin tunneling asymmetry. All other plotting parameters are the same as those in Fig. 2.

Finally, we investigate the difference between the stationary entropy production rate evaluated by our GQME approach and BMS master equation. As mentioned in Sec. III, the BMS master equation can be obtained by neglecting the last six lines of Eq. (16), which is justified when the terms in the last six lines of Eq. (A23) experience fast oscillations and very rapidly average to zero. The entropy associated with the reduced density matrix in the BMS master equation $\rho^{BMS}(t)$ simply reads

$$S^{BMS}(t) = -\mathrm{tr}_S[\rho^{BMS}\ln\rho^{BMS}] = S_i^{BMS} + S_e^{BMS}, \tag{59}$$

where S_i^{BMS} is entropy production and $S_e^{BMS} = \beta Q^{BMS}$ is the entropy flow, with Q^{BMS} the heat flow evaluated based in the BMS master equation. Following a similar procedure in Sec. IV A, the average heat flow in the stationary limit can be readily evaluated as

$$\dot{Q}^{BMS} = \frac{\Omega}{2}J_{sp}^{BMS} = \frac{\Omega}{2}(J_\uparrow^{BMS} - J_\downarrow^{BMS}), \tag{60}$$

where J_{sp}^{BMS} is the stationary net spin current obtained using BMS master equation, with individual spin-σ ($\sigma = \uparrow, \downarrow$) component given by

$$J_\sigma^{BMS} = \Gamma_{0,+}^{(\sigma)}\rho_{++}^{BMS} + \Gamma_{0,-}^{(\sigma)}\rho_{--}^{BMS} - \left[\Gamma_{+,0}^{(\sigma)} + \Gamma_{-,0}^{(\sigma)}\right]\rho_{00}^{BMS}. \tag{61}$$

Here, $\rho_{jj}^{BMS} = \langle u_j(t)|\rho^{BMS}(t)|u_j(t)\rangle$ ($j \in \{0, +, -\}$) are the matrix elements of the BMS master equation in the Floquet basis.

In the stationary limit, the rate of entropy change in the system vanishes ($\dot{S}^{BMS} = 0$); the corresponding entropy production rate reads

$$\dot{S}_i^{BMS} = -\beta\dot{Q}^{MBS} = -\frac{\beta\Omega}{2}J_{sp}^{BMS}. \tag{62}$$

Eventually, one obtains the difference between the stationary entropy production rate evaluated by our GQME approach and BMS master equation

$$\dot{S}_i - \dot{S}_i^{BMS} = -\frac{\beta\Omega}{2}\left(J_{sp}^{st} - J_{sp}^{BMS}\right) + \frac{\beta\Lambda}{2}J_X^{st}. \tag{63}$$

Apparently, the difference comes from two contributions. The first one is due to the difference of the net spin currents for the two cases. The second contribution originates from the interaction between the accumulated average spin and the effective magnetic field.

To clearly demonstrate this difference, in Fig. 7 we plot $(\dot{S}_i - \dot{S}_i^{BMS})$ versus Rabi frequency for different configurations of spin tunneling asymmetry. For symmetric tunneling ($\Gamma_\uparrow = \Gamma_\downarrow = 0.5\Gamma$), the occupation of the QD obtained from the two approaches is very close to each other, see Fig. 3. Furthermore, the contribution from the second term in Eq. (63) is negligible, cf. Fig. 4(a). This leads to an almost vanishing difference between $\dot{S}_i$ and $\dot{S}_i^{BMS}$, as indicated by the solid curve in Fig. 7. As the asymmetry grows, the contribution from the interaction between the average spin and the effective magnetic field will have an increasing role to play. For a very asymmetric spin tunneling ($\Gamma_\uparrow = 0.05\Gamma$, $\Gamma_\downarrow = 0.95\Gamma$), one observes a noticeable difference, which could be close to the magnitude of $\dot{S}_i$ itself by comparing with the energy current in Fig. 4(d). (Note we take $\beta\Gamma = 0.1$ in plotting Fig. 7.) A further investigation reveals that the major contribution to the difference arises from the interaction between the average spin and the effective magnetic field. At this point, we thus emphasize the importance of using a GQME, especially for the case of very asymmetric spin tunneling rates, as the using of a BMS master equation may lead to an underestimation of the entropy production. Finally, we remark that the contribution from J_X^{st} is of the first order in tunnel-coupling strength and thus could be detected in experiment. We highly anticipate this to be verified in the near future.

V. CONCLUSION

In summary, we have performed a stochastic thermodynamics analysis of an ESR pumped quantum dot system in the presence of a pure spin current only. The state of the system can be described by populations and an average spin in the Floquet basis. In particular, this average spin undergoes a precession about an effective magnetic field, which originates from the nonsecular treatment and energy

renormalization. Unambiguously, an energy current could be generated, not due to a charge current, but entailed by a pure spin current and the interaction between average spin and effective magnetic field, where the latter have the dominant role to play in the case of strong asymmetry in spin tunneling. In the stationary limit, energy balance and entropy balance relations are established based on the theory of counting statistics. Furthermore, we revealed a mechanism that the irreversible entropy production is found to be intimately related to the interaction between average spin and magnetic field.

ACKNOWLEDGMENTS

We would like to thank S. K. Wang for fruitful discussion. Support from the National Natural Science Foundation of China (Grant Nos. 11774311 and 11647082) and education department of Zhejiang Province (No. 8) is gratefully acknowledged.

APPENDIX: DERIVATION OF THE GQME

First, we transform from the Schrödinger's picture to the interaction picture

$$\tilde{\rho}_{\rm T}(\boldsymbol{\chi},t)=U_0^{\dagger}(t)\rho_{\rm T}(\boldsymbol{\chi},t)U_0(t), \tag{A1}$$

where

$$U_0(t)\equiv \exp_+\left\{-{\rm i}\int_0^t {\rm d}\tau H_{\rm S}(\tau)\right\}e^{-{\rm i}H_{\rm B}t}. \tag{A2}$$

In what follows, the tilde is used to indicate a quantity in the interaction picture. The equation of motion of $\tilde{\rho}_{\rm T}(\boldsymbol{\chi},t)$ then reads

$$\frac{\rm d}{{\rm d}t}\tilde{\rho}_{\rm T}(\boldsymbol{\chi},t)=-{\rm i}\{\tilde{V}(\boldsymbol{\chi},t)\tilde{\rho}_{\rm T}(\boldsymbol{\chi},t)-\tilde{\rho}_{\rm T}(\boldsymbol{\chi},t)\tilde{V}(-\boldsymbol{\chi},t)\}, \tag{A3}$$

with

$$\tilde{V}(\boldsymbol{\chi},t)=U_0^{\dagger}(t)V(\boldsymbol{\chi})U_0(t). \tag{A4}$$

Now, we integrate Eq. (A3) twice, differentiate with respect to time "t," and trace over the degrees of freedom of the reservoir. This yields an exact equation of motion for the $\boldsymbol{\chi}$-dependent reduced density matrix

$$\begin{aligned}\frac{\rm d}{{\rm d}t}\tilde{\rho}(\boldsymbol{\chi},t)=&-\int_0^t {\rm d}\tau\ {\rm tr}_{\rm B}\{\tilde{V}(\boldsymbol{\chi},t)\tilde{V}(\boldsymbol{\chi},\tau)\tilde{\rho}_{\rm T}(\boldsymbol{\chi},\tau)\\&-\tilde{V}(\boldsymbol{\chi},\tau)\tilde{\rho}_{\rm T}(\boldsymbol{\chi},\tau)\tilde{V}(-\boldsymbol{\chi},t)\\&-\tilde{V}(\boldsymbol{\chi},t)\tilde{\rho}_{\rm T}(\boldsymbol{\chi},\tau)\tilde{V}(-\boldsymbol{\chi},\tau)\\&+\tilde{\rho}_{\rm T}(\boldsymbol{\chi},\tau)\tilde{V}(-\boldsymbol{\chi},\tau)\tilde{V}(-\boldsymbol{\chi},t)\},\end{aligned} \tag{A5}$$

where ${\rm tr}_{\rm B}\{\cdots\}$ stands for the trace over the degrees of freedom of reservoir. This equation still contains the density matrix $\tilde{\rho}_{\rm T}(\boldsymbol{\chi},\tau)$ of the entire system. We thus now make the Born approximation which assumes that the density operator factorizes at all times as $\tilde{\rho}_{\rm T}(\boldsymbol{\chi},\tau)=\tilde{\rho}(\boldsymbol{\chi},\tau)\otimes\rho_{\rm B}$. It greatly simplifies Eq. (A5). Yet, it still has a time nonlocal form: The future evolution $\tilde{\rho}(\boldsymbol{\chi},t)$ depends on its past history $\tilde{\rho}(\boldsymbol{\chi},\tau)$, which makes it difficult to work with. In case of a large separation between system and environment timescales, it is justified to introduce the Markov approximation, i.e., replacing $\tilde{\rho}(\boldsymbol{\chi},\tau)$ by $\tilde{\rho}(\boldsymbol{\chi},t)$ and extending the upper limit of the integral to infinity in Eq. (A5). Finally, it yields a closed differential equation of motion for the reduced density matrix that the future behavior of $\tilde{\rho}(\boldsymbol{\chi},t)$ depends only on its present state

$$\begin{aligned}\frac{\rm d}{{\rm d}t}\tilde{\rho}(\boldsymbol{\chi},t)=&-\int_0^{\infty}{\rm d}\tau{\rm tr}_{\rm B}\{\tilde{V}(\boldsymbol{\chi},t)\tilde{V}(\boldsymbol{\chi},t-\tau)\rho_{\rm B}\otimes\tilde{\rho}(\boldsymbol{\chi},t)\\&-\tilde{V}(\boldsymbol{\chi},t-\tau)\rho_{\rm B}\otimes\tilde{\rho}(\boldsymbol{\chi},t)\tilde{V}(-\boldsymbol{\chi},t)\\&-\tilde{V}(\boldsymbol{\chi},t)\rho_{\rm B}\otimes\tilde{\rho}(\boldsymbol{\chi},t)\tilde{V}(-\boldsymbol{\chi},t-\tau)\\&+\rho_{\rm B}\otimes\tilde{\rho}(\boldsymbol{\chi},t)\tilde{V}(-\boldsymbol{\chi},t-\tau)\tilde{V}(-\boldsymbol{\chi},t)\}\\=&-\{[{\rm I}]-[{\rm II}]-[{\rm III}]+[{\rm IV}]\}.\end{aligned} \tag{A6}$$

This serves as an essential starting point for the following derivation.

Each term in Eq. (A6) has to be evaluated, which requires the explicit form of $V(\boldsymbol{\chi},t)$ in Eq. (A4). By utilizing Eqs. (13) and (A2), one immediately has

$$\begin{aligned}\tilde{f}_{\sigma}(\boldsymbol{\chi},t)=&U_0^{\dagger}(t)f_{\sigma}(\boldsymbol{\chi})U_0(t)\\=&\sum_k t_{k\sigma}c_{k\sigma}e^{-\frac{\rm i}{2}(\chi_{2\sigma}\varepsilon_{k\sigma}+\chi_{1\sigma})}e^{-{\rm i}\varepsilon_{k\sigma}t}.\end{aligned} \tag{A7}$$

The system operators in the interaction picture are defined analogously

$$\begin{aligned}\tilde{d}_{\sigma}(t)=&U_0^{\dagger}(t)d_{\sigma}(t)U_0(t)\\=&\exp_-\left\{{\rm i}\int_0^t H_{\rm S}(\tau)d\tau\right\}d_{\sigma}\exp_+\left\{-{\rm i}\int_0^t H_{\rm S}(\tau)d\tau\right\},\end{aligned} \tag{A8}$$

where the time ordering arises purely from the time dependence of the system Hamiltonian. To explicitly evaluate Eq. (A8), we employ Floquet theory [48–51], which states that the unitary evolution can be represented as

$$\exp_+\left\{-{\rm i}\int_0^t H_{\rm S}(\tau)d\tau\right\}=\sum_j e^{-{\rm i}\epsilon_j t}|u_j(t)\rangle\langle u_j(0)|, \tag{A9}$$

where $|u_j(t)\rangle$ is the Floquet function inheriting the periodicity $|u_j(t)\rangle=|u_j(t+T)\rangle$ with $T=\frac{2\pi}{\Omega}$, and ϵ_j is the corresponding quasienergy. The quasienergies and Floquet functions are simply given, respectively, by

$$\epsilon_0=0,\quad |u_0(t)\rangle=\begin{pmatrix}1\\0\\0\end{pmatrix}, \tag{A10a}$$

$$\epsilon_+=\frac{\Omega+\Lambda}{2},\quad |u_+(t)\rangle=\begin{pmatrix}0\\\sin\left(\frac{\Theta}{2}\right)\\\cos\left(\frac{\Theta}{2}\right)e^{{\rm i}\Omega t}\end{pmatrix}, \tag{A10b}$$

$$\epsilon_-=\frac{\Omega-\Lambda}{2},\quad |u_-(t)\rangle=\begin{pmatrix}0\\-\cos\left(\frac{\Theta}{2}\right)\\\sin\left(\frac{\Theta}{2}\right)e^{{\rm i}\Omega t}\end{pmatrix}, \tag{A10c}$$

where, for brevity, we have introduced

$$\sin\left(\frac{\Theta}{2}\right)=\sqrt{\frac{\Lambda+\delta}{2\Lambda}}, \tag{A11a}$$

$$\cos\left(\frac{\Theta}{2}\right)=\sqrt{\frac{\Lambda-\delta}{2\Lambda}}, \tag{A11b}$$

where $\delta=\Delta-\Omega$ is the ESR detuning and $\Lambda=\sqrt{\delta^2+4\gamma_{\rm RF}^2}$. The annihilation operators of the system in the Floquet basis can thus be readily expressed as

$$\tilde{d}_\uparrow(t)=\sin\left(\frac{\Theta}{2}\right)e^{-\mathrm{i}(\epsilon_+-\epsilon_0-\frac{\Omega}{2})t}|u_0(0)\rangle\langle u_+(0)|-\cos\left(\frac{\Theta}{2}\right)e^{-\mathrm{i}(\epsilon_--\epsilon_0-\frac{\Omega}{2})t}|u_0(0)\rangle\langle u_-(0)|, \tag{A12a}$$

$$\tilde{d}_\downarrow(t)=\cos\left(\frac{\Theta}{2}\right)e^{-\mathrm{i}(\epsilon_+-\epsilon_0+\frac{\Omega}{2})t}|u_0(0)\rangle\langle u_+(0)|+\sin\left(\frac{\Theta}{2}\right)e^{-\mathrm{i}(\epsilon_--\epsilon_0+\frac{\Omega}{2})t}|u_0(0)\rangle\langle u_-(0)|. \tag{A12b}$$

Their corresponding creation operators can be obtained by simply taking the Hermitian conjugate.

The following procedure relies on the substituting of Eqs. (A7) and (A12) into Eq. (A6). For instance, the first term [I] in Eq. (A6) is obtained as

$$\begin{aligned}
[\mathrm{I}]=&\left\{\gamma_\downarrow^{(+)}\left(\epsilon_+-\epsilon_0+\frac{\Omega}{2}\right)\cos^2\left(\frac{\Theta}{2}\right)+\gamma_\uparrow^{(+)}\left(\epsilon_+-\epsilon_0-\frac{\Omega}{2}\right)\sin^2\left(\frac{\Theta}{2}\right)\right\}|u_0(0)\rangle\,\langle u_0(0)|\,\tilde{\rho}(\boldsymbol{\chi},t)\\
&+\left\{\gamma_\downarrow^{(+)}\left(\epsilon_--\epsilon_0+\frac{\Omega}{2}\right)\sin^2\left(\frac{\Theta}{2}\right)+\gamma_\uparrow^{(+)}\left(\epsilon_--\epsilon_0-\frac{\Omega}{2}\right)\cos^2\left(\frac{\Theta}{2}\right)\right\}|u_0(0)\rangle\,\langle u_0(0)|\,\tilde{\rho}(\boldsymbol{\chi},t)\\
&+\left\{\gamma_\downarrow^{(-)}\left(\epsilon_+-\epsilon_0+\frac{\Omega}{2}\right)\cos^2\left(\frac{\Theta}{2}\right)+\gamma_\uparrow^{(-)}\left(\epsilon_+-\epsilon_0-\frac{\Omega}{2}\right)\sin^2\left(\frac{\Theta}{2}\right)\right\}|u_+(0)\rangle\langle u_+(0)|\tilde{\rho}(\boldsymbol{\chi},t)\\
&+\left\{\gamma_\downarrow^{(-)}\left(\epsilon_--\epsilon_0+\frac{\Omega}{2}\right)\sin^2\left(\frac{\Theta}{2}\right)+\gamma_\uparrow^{(-)}\left(\epsilon_--\epsilon_0-\frac{\Omega}{2}\right)\cos^2\left(\frac{\Theta}{2}\right)\right\}|u_-(0)\rangle\langle u_-(0)|\tilde{\rho}(\boldsymbol{\chi},t)\\
&+\frac{1}{2}\sin\Theta\,e^{+\mathrm{i}(\epsilon_+-\epsilon_-)t}\left\{\gamma_\downarrow^{(-)}\left(\epsilon_--\epsilon_0+\frac{\Omega}{2}\right)-\gamma_\uparrow^{(-)}\left(\epsilon_--\epsilon_0-\frac{\Omega}{2}\right)\right\}|u_+(0)\rangle\langle u_-(0)|\tilde{\rho}(\boldsymbol{\chi},t)\\
&+\frac{1}{2}\sin\Theta\,e^{-\mathrm{i}(\epsilon_+-\epsilon_-)t}\left\{\gamma_\downarrow^{(-)}\left(\epsilon_+-\epsilon_0+\frac{\Omega}{2}\right)-\gamma_\uparrow^{(-)}\left(\epsilon_+-\epsilon_0-\frac{\Omega}{2}\right)\right\}|u_-(0)\rangle\langle u_+(0)|\tilde{\rho}(\boldsymbol{\chi},t).
\end{aligned} \tag{A13}$$

The term [IV] in Eq. (A6) can be analyzed in a similar way.

We have introduced

$$\gamma_\sigma^{(\pm)}(\omega)=\sum_k\int_0^\infty \mathrm{d}\tau e^{-\mathrm{i}\omega\tau}C_\sigma^{(\pm)}(\tau), \tag{A14}$$

where $C_\sigma^{(\pm)}(\tau)$ are the reservoir correlation functions defined as

$$C_\sigma^{(+)}(\tau)=\langle\tilde{f}_\sigma^\dagger(\tau)\tilde{f}_\sigma(0)\rangle_{\rm B}, \tag{A15a}$$

$$C_\sigma^{(-)}(\tau)=\langle\tilde{f}_\sigma(\tau)\tilde{f}_\sigma^\dagger(0)\rangle_{\rm B}, \tag{A15b}$$

with $\tilde{f}_\sigma(\tau)\equiv\tilde{f}_\sigma(\boldsymbol{\chi}=\mathbf{0},\tau)$ and $\langle(\cdots)\rangle_{\rm B}\equiv\mathrm{tr}_{\rm B}[(\cdots)\rho_{\rm B}]$ the usual thermal average. By substituting Eq. (A7) into Eq. (A15), the reservoir correlation functions simplify to

$$C_\sigma^{(\pm)}(\tau)=\sum_k|t_{k\sigma}|^2f^{(\pm)}(\varepsilon_{k\sigma})e^{\pm\mathrm{i}\varepsilon_{k\sigma}\tau}. \tag{A16}$$

Actually, Eq. (A14) is a causality transformation, which can be decomposed into spectral functions and dispersion functions as [73]

$$\gamma_\sigma^{(\pm)}(\omega)=\Gamma_\sigma^{(\pm)}(\omega)+\mathrm{i}D_\sigma^{(\pm)}(\omega). \tag{A17}$$

The involved spectral functions are simply the Fourier transforms of the corresponding reservoir correlation functions

$$\Gamma_\sigma^{(\pm)}(\omega)=\int_{-\infty}^\infty \mathrm{d}\tau e^{-\mathrm{i}\omega\tau}C_\sigma^{(\pm)}(\tau). \tag{A18}$$

In the usual wide-band limit, it reduces to

$$\Gamma_\sigma^{(\pm)}(\omega)=\Gamma_\sigma f^{(\pm)}(\omega), \tag{A19}$$

where Γ_σ is the tunneling width, $f^{(+)}(\omega)$ is the usual Fermi function, and $f^{(-)}(\omega)\equiv1-f^{(+)}(\omega)$. With the knowledge of the spectral functions, the dispersion functions in Eq. (A17) can be obtained via the Kramers-Kronig relation [73,74]

$$D_\sigma^{(\pm)}(\omega)=-\frac{1}{\pi}\mathcal{P}\int_{-\infty}^\infty \mathrm{d}\omega'\frac{C_\sigma^{(\pm)}(\omega')}{\omega-\omega'}, \tag{A20}$$

where $\mathcal{P}$ denotes the principle value. By introducing a Lorentzian cutoff $J(\omega)=\frac{\mathrm{w}^2}{(\omega-\mu_0)^2+\mathrm{w}^2}$ centered at $\omega=\mu_0$ and with bandwidth w, the dispersion functions can be evaluated

$$D_\sigma^{(\pm)}(\omega)=\pm\frac{\Gamma_\sigma}{\pi}\left\{\ln\left(\frac{\beta\mathrm{w}}{2\pi}\right)-\mathrm{Re}\Psi\left[\frac{1}{2}+\frac{\mathrm{i}\beta}{2\pi}(\omega-\mu_0)\right]\right\}, \tag{A21}$$

where $\Psi(x)$ is the digamma function. The dispersion functions normally account for the system-bath coupling-induced energy renormalization, similar to the so-called Lamb shift. It has been revealed that the energy renormalization have strong influence on electron transport through QD systems [75–77], Aharonov-Bohm interferometer [78,79], quantum measurement of solid-state qubit [80,81]. Later, we will show that the dispersion functions in ESR pumping have important contribution to an effective magnetic field.

It is noted that in Eq. (A13) the coefficients are independent of the counting fields. Mathematically, this is due to fact that for nonzero reservoir correlation functions, one should only account for the thermal averages of $\tilde{f}_\sigma(\boldsymbol{\chi})$ and its Hermitian conjugate with the same momentum and spin, cf. Eq. (A15). Physically, this implies that the term [I] in Eq. (A13) is not directly responsible for particle and energy transport. However, it does not necessarily mean that they do not have any contribution. Actually, they may have important roles to play via influencing the spin dynamics. Similar analysis applies to the last term [IV] in Eq. (A6), which is also $\boldsymbol{\chi}$ independent. This is no longer the case for the second and third terms, i.e., [II] and [III] in Eq. (A6), which depend explicitly on the counting fields. For instance, the term [II] is given by

$$
\begin{aligned}
[\mathrm{II}] = &\left\{\gamma_\downarrow^{(+)}\left(\epsilon_+ - \epsilon_0 + \frac{\Omega}{2}\right)\cos^2\left(\frac{\Theta}{2}\right)e^{-\mathrm{i}(\epsilon_+-\epsilon_0+\frac{\Omega}{2})\chi_{2\downarrow}-\mathrm{i}\chi_{1\downarrow}} + \gamma_\uparrow^{(+)}\left(\epsilon_+ - \epsilon_0 - \frac{\Omega}{2}\right)\sin^2\left(\frac{\Theta}{2}\right)e^{-\mathrm{i}(\epsilon_+-\epsilon_0-\frac{\Omega}{2})\chi_{2\uparrow}-\mathrm{i}\chi_{1\uparrow}}\right\}\\
&\times |u_+(0)\rangle\langle u_0(0)|\tilde{\rho}(\boldsymbol{\chi},t)|u_0(0)\rangle\langle u_+(0)|\\
&+\left\{\gamma_\downarrow^{(+)}\left(\epsilon_- - \epsilon_0 + \frac{\Omega}{2}\right)\sin^2\left(\frac{\Theta}{2}\right)e^{-\mathrm{i}(\epsilon_--\epsilon_0+\frac{\Omega}{2})\chi_{2\downarrow}-\mathrm{i}\chi_{1\downarrow}} + \gamma_\uparrow^{(+)}\left(\epsilon_- - \epsilon_0 - \frac{\Omega}{2}\right)\cos^2\left(\frac{\Theta}{2}\right)e^{-\mathrm{i}(\epsilon_--\epsilon_0-\frac{\Omega}{2})\chi_{2\uparrow}-\mathrm{i}\chi_{1\uparrow}}\right\}\\
&\times |u_-(0)\rangle\langle u_0(0)|\tilde{\rho}(\boldsymbol{\chi},t)|u_0(0)\rangle\langle u_-(0)|\\
&+\left\{\gamma_\downarrow^{(-)}\left(\epsilon_+ - \epsilon_0 + \frac{\Omega}{2}\right)\cos^2\left(\frac{\Theta}{2}\right)e^{+\mathrm{i}(\epsilon_+-\epsilon_0+\frac{\Omega}{2})\chi_{2\downarrow}+\mathrm{i}\chi_{1\downarrow}} + \gamma_\uparrow^{(-)}\left(\epsilon_+ - \epsilon_0 - \frac{\Omega}{2}\right)\sin^2\left(\frac{\Theta}{2}\right)e^{+\mathrm{i}(\epsilon_+-\epsilon_0-\frac{\Omega}{2})\chi_{2\uparrow}+\mathrm{i}\chi_{1\uparrow}}\right\}\\
&\times |u_0(0)\rangle\langle u_+(0)|\tilde{\rho}(\boldsymbol{\chi},t)|u_+(0)\rangle\langle u_0(0)|\\
&+\left\{\gamma_\downarrow^{(-)}\left(\epsilon_- - \epsilon_0 + \frac{\Omega}{2}\right)\sin^2\left(\frac{\Theta}{2}\right)e^{+\mathrm{i}(\epsilon_--\epsilon_0+\frac{\Omega}{2})\chi_{2\downarrow}+\mathrm{i}\chi_{1\downarrow}} + \gamma_\uparrow^{(-)}\left(\epsilon_- - \epsilon_0 - \frac{\Omega}{2}\right)\cos^2\left(\frac{\Theta}{2}\right)e^{+\mathrm{i}(\epsilon_--\epsilon_0-\frac{\Omega}{2})\chi_{2\uparrow}+\mathrm{i}\chi_{1\uparrow}}\right\}\\
&\times |u_0(0)\rangle\langle u_-(0)|\tilde{\rho}(\boldsymbol{\chi},t)|u_-(0)\rangle\langle u_0(0)|\\
&+\frac{1}{2}\sin\Theta\, e^{+\mathrm{i}(\epsilon_+-\epsilon_-)t}\left\{\gamma_\downarrow^{(+)}\left(\epsilon_+ - \epsilon_0 + \frac{\Omega}{2}\right)e^{-\mathrm{i}(\epsilon_+-\epsilon_0+\frac{\Omega}{2})\chi_{2\downarrow}-\mathrm{i}\chi_{1\downarrow}} - \gamma_\uparrow^{(+)}\left(\epsilon_+ - \epsilon_0 - \frac{\Omega}{2}\right)e^{-\mathrm{i}(\epsilon_+-\epsilon_0-\frac{\Omega}{2})\chi_{2\uparrow}-\mathrm{i}\chi_{1\uparrow}}\right\}\\
&\times |u_+(0)\rangle\langle u_0(0)|\tilde{\rho}(\boldsymbol{\chi},t)|u_0(0)\rangle\langle u_-(0)|\\
&+\frac{1}{2}\sin\Theta\, e^{-\mathrm{i}(\epsilon_+-\epsilon_-)t}\left\{\gamma_\downarrow^{(+)}\left(\epsilon_- - \epsilon_0 + \frac{\Omega}{2}\right)e^{-\mathrm{i}(\epsilon_--\epsilon_0+\frac{\Omega}{2})\chi_{2\downarrow}-\mathrm{i}\chi_{1\downarrow}} - \gamma_\uparrow^{(+)}\left(\epsilon_- - \epsilon_0 - \frac{\Omega}{2}\right)e^{-\mathrm{i}(\epsilon_--\epsilon_0-\frac{\Omega}{2})\chi_{2\uparrow}-\mathrm{i}\chi_{1\uparrow}}\right\}\\
&\times |u_-(0)\rangle\langle u_0(0)|\tilde{\rho}(\boldsymbol{\chi},t)|u_0(0)\rangle\langle u_+(0)|\\
&+\frac{1}{2}\sin\Theta\, e^{-\mathrm{i}(\epsilon_+-\epsilon_-)t}\left\{\gamma_\downarrow^{(-)}\left(\epsilon_+ - \epsilon_0 + \frac{\Omega}{2}\right)e^{+\mathrm{i}(\epsilon_+-\epsilon_0+\frac{\Omega}{2})\chi_{2\downarrow}+\mathrm{i}\chi_{1\downarrow}} - \gamma_\uparrow^{(-)}\left(\epsilon_+ - \epsilon_0 - \frac{\Omega}{2}\right)e^{+\mathrm{i}(\epsilon_+-\epsilon_0-\frac{\Omega}{2})\chi_{2\uparrow}+\mathrm{i}\chi_{1\uparrow}}\right\}\\
&\times |u_0(0)\rangle\langle u_+(0)|\tilde{\rho}(\boldsymbol{\chi},t)|u_-(0)\rangle\langle u_0(0)|\\
&+\frac{1}{2}\sin\Theta\, e^{+\mathrm{i}(\epsilon_+-\epsilon_-)t}\left\{\gamma_\downarrow^{(-)}\left(\epsilon_- - \epsilon_0 + \frac{\Omega}{2}\right)e^{+\mathrm{i}(\epsilon_--\epsilon_0+\frac{\Omega}{2})\chi_{2\downarrow}+\mathrm{i}\chi_{1\downarrow}} - \gamma_\uparrow^{(-)}\left(\epsilon_- - \epsilon_0 - \frac{\Omega}{2}\right)e^{+\mathrm{i}(\epsilon_--\epsilon_0-\frac{\Omega}{2})\chi_{2\uparrow}+\mathrm{i}\chi_{1\uparrow}}\right\}\\
&\times |u_0(0)\rangle\langle u_-(0)|\tilde{\rho}(\boldsymbol{\chi},t)|u_+(0)\rangle\langle u_0(0)|. \qquad \text{(A22)}
\end{aligned}
$$

Accordingly, the term [III] can be obtained following the similar procedure. By putting all four terms in Eq. (A6) together, one finally arrive at the GQME in the interaction picture as

$$
\begin{aligned}
\frac{\mathrm{d}}{\mathrm{d}t}\tilde{\rho}(\boldsymbol{\chi},t) = &\left\{\Gamma_{0,+}(\boldsymbol{\chi})\mathcal{J}[|u_0(0)\rangle\langle u_+(0)|] - \frac{1}{2}\Gamma_{0,+}\mathcal{A}[|u_0(0)\rangle\langle u_+(0)|] - \frac{\mathrm{i}}{2}\kappa_{0,+}\mathcal{C}[|u_0(0)\rangle\langle u_+(0)|]\right\}\tilde{\rho}(\boldsymbol{\chi},t)\\
&+\left\{\Gamma_{0,-}(\boldsymbol{\chi})\mathcal{J}[|u_0(0)\rangle\langle u_-(0)|] - \frac{1}{2}\Gamma_{0,-}\mathcal{A}[|u_0(0)\rangle\langle u_-(0)|] - \frac{\mathrm{i}}{2}\kappa_{0,-}\mathcal{C}[|u_0(0)\rangle\langle u_-(0)|]\right\}\tilde{\rho}(\boldsymbol{\chi},t)\\
&+\left\{\Gamma_{+,0}(\boldsymbol{\chi})\mathcal{J}[|u_+(0)\rangle\langle u_0(0)|] - \frac{1}{2}\Gamma_{+,0}\mathcal{A}[|u_+(0)\rangle\langle u_0(0)|] - \frac{\mathrm{i}}{2}\kappa_{+,0}\mathcal{C}[|u_+(0)\rangle\langle u_0(0)|]\right\}\tilde{\rho}(\boldsymbol{\chi},t)\\
&+\left\{\Gamma_{-,0}(\boldsymbol{\chi})\mathcal{J}[|u_-(0)\rangle\langle u_0(0)|] - \frac{1}{2}\Gamma_{-,0}\mathcal{A}[|u_-(0)\rangle\langle u_0(0)|] - \frac{\mathrm{i}}{2}\kappa_{-,0}\mathcal{C}[|u_-(0)\rangle\langle u_0(0)|]\right\}\tilde{\rho}(\boldsymbol{\chi},t)
\end{aligned}
$$

$$
\begin{aligned}
&- e^{+\mathrm{i}(\epsilon_+-\epsilon_-)t}\{[\Upsilon_{0,-}+\mathrm{i}\xi_{0,-}]|u_+(0)\rangle\langle u_-(0)|\tilde{\rho}(\boldsymbol{\chi},t)+[\Upsilon_{0,+}-\mathrm{i}\xi_{0,+}]\tilde{\rho}(\boldsymbol{\chi},t)|u_+(0)\rangle\langle u_-(0)|\}\\
&- e^{-\mathrm{i}(\epsilon_+-\epsilon_-)t}\{[\Upsilon_{0,+}+\mathrm{i}\xi_{0,+}]|u_-(0)\rangle\langle u_+(0)|\tilde{\rho}(\boldsymbol{\chi},t)+[\Upsilon_{0,-}-\mathrm{i}\xi_{0,-}]\tilde{\rho}(\boldsymbol{\chi},t)|u_-(0)\rangle\langle u_+(0)|\}\\
&+ e^{+\mathrm{i}(\epsilon_+-\epsilon_-)t}[\Upsilon_{+,0}(\boldsymbol{\chi})+\mathrm{i}\xi_{+,0}(\boldsymbol{\chi})+\Upsilon_{-,0}(\boldsymbol{\chi})-\mathrm{i}\xi_{-,0}(\boldsymbol{\chi})]|u_+(0)\rangle\langle u_0(0)|\tilde{\rho}(\boldsymbol{\chi},t)|u_0(0)\rangle\langle u_-(0)|\\
&+ e^{+\mathrm{i}(\epsilon_+-\epsilon_-)t}[\Upsilon_{0,+}(\boldsymbol{\chi})-\mathrm{i}\xi_{0,+}(\boldsymbol{\chi})+\Upsilon_{0,-}(\boldsymbol{\chi})+\mathrm{i}\xi_{0,-}(\boldsymbol{\chi})]|u_0(0)\rangle\langle u_-(0)|\tilde{\rho}(\boldsymbol{\chi},t)|u_+(0)\rangle\langle u_0(0)|\\
&+ e^{-\mathrm{i}(\epsilon_+-\epsilon_-)t}[\Upsilon_{+,0}(\boldsymbol{\chi})-\mathrm{i}\xi_{+,0}(\boldsymbol{\chi})+\Upsilon_{-,0}(\boldsymbol{\chi})+\mathrm{i}\xi_{-,0}(\boldsymbol{\chi})]|u_-(0)\rangle\langle u_0(0)|\tilde{\rho}(\boldsymbol{\chi},t)|u_0(0)\rangle\langle u_+(0)|\\
&+ e^{-\mathrm{i}(\epsilon_+-\epsilon_-)t}[\Upsilon_{0,+}(\boldsymbol{\chi})+\mathrm{i}\xi_{0,+}(\boldsymbol{\chi})+\Upsilon_{0,-}(\boldsymbol{\chi})-\mathrm{i}\xi_{0,-}(\boldsymbol{\chi})]|u_0(0)\rangle\langle u_+(0)|\tilde{\rho}(\boldsymbol{\chi},t)|u_-(0)\rangle\langle u_0(0)|, \qquad \text{(A23)}
\end{aligned}
$$

where we have introduced the superoperators $\mathcal{J}[r]\rho = r\rho r^\dagger$, $\mathcal{A}[r]\rho = r^\dagger r\rho + \rho r^\dagger r$, and $\mathcal{C}[r]\rho = [r^\dagger r, \rho]$.

The first four lines in Eq. (A23) depict the tunneling between QD and side reservoir in the Lindblad-like form, where the $\boldsymbol{\chi}$-dependent terms are directly responsible for particle and energy transfer. The involved $\boldsymbol{\chi}$-dependent rates are given by

$$
\begin{aligned}
\Gamma_{0,\pm}(\boldsymbol{\chi}) &= \Gamma_{0,\pm}^{(\downarrow)} e^{+\mathrm{i}(\epsilon_\pm-\epsilon_0+\frac{\Omega}{2})\chi_{2\downarrow}+\mathrm{i}\chi_{1\downarrow}}\\
&\quad + \Gamma_{0,\pm}^{(\uparrow)} e^{+\mathrm{i}(\epsilon_\pm-\epsilon_0-\frac{\Omega}{2})\chi_{2\uparrow}+\mathrm{i}\chi_{1\uparrow}}, \qquad \text{(A24a)}\\
\Gamma_{\pm,0}(\boldsymbol{\chi}) &= \Gamma_{\pm,0}^{(\downarrow)} e^{-\mathrm{i}(\epsilon_\pm-\epsilon_0+\frac{\Omega}{2})\chi_{2\downarrow}-\mathrm{i}\chi_{1\downarrow}}\\
&\quad + \Gamma_{\pm,0}^{(\uparrow)} e^{-\mathrm{i}(\epsilon_\pm-\epsilon_0-\frac{\Omega}{2})\chi_{2\uparrow}-\mathrm{i}\chi_{1\uparrow}}, \qquad \text{(A24b)}
\end{aligned}
$$

with

$$
\begin{aligned}
\Gamma_{0,\pm}^{(\downarrow)} &= \frac{1\pm\cos\Theta}{2}\Gamma_\downarrow^{(-)}\left(\epsilon_\pm-\epsilon_0+\frac{\Omega}{2}\right), \qquad \text{(A25a)}\\
\Gamma_{0,\pm}^{(\uparrow)} &= \frac{1\mp\cos\Theta}{2}\Gamma_\uparrow^{(-)}\left(\epsilon_\pm-\epsilon_0-\frac{\Omega}{2}\right), \qquad \text{(A25b)}\\
\Gamma_{\pm,0}^{(\downarrow)} &= \frac{1\pm\cos\Theta}{2}\Gamma_\downarrow^{(+)}\left(\epsilon_\pm-\epsilon_0+\frac{\Omega}{2}\right), \qquad \text{(A25c)}\\
\Gamma_{\pm,0}^{(\uparrow)} &= \frac{1\mp\cos\Theta}{2}\Gamma_\uparrow^{(+)}\left(\epsilon_\pm-\epsilon_0-\frac{\Omega}{2}\right). \qquad \text{(A25d)}
\end{aligned}
$$

The spectral functions $\Gamma_\sigma^{(\pm)}(\omega)$ are given in Eq. (A18). The corresponding $\boldsymbol{\chi}$-independent rates are simply obtained by setting $\boldsymbol{\chi} = \mathbf{0}$, i.e., $\Gamma_{0,\pm} = \Gamma_{0,\pm}(\boldsymbol{\chi}=\mathbf{0})$, and likewise for $\Gamma_{\pm,0}$. The terms $\kappa_{0,\pm}$ and $\kappa_{\pm,0}$ are only related to energy renormalization and thus not involved in particle and energy transport. They do not depend on the counting fields

$$
\begin{aligned}
\kappa_{0,\pm} &= \frac{1\pm\cos\Theta}{2}D_\downarrow^{(-)}\left(\epsilon_\pm-\epsilon_0+\frac{\Omega}{2}\right)\\
&\quad + \frac{1\mp\cos\Theta}{2}D_\uparrow^{(-)}\left(\epsilon_\pm-\epsilon_0-\frac{\Omega}{2}\right), \qquad \text{(A26a)}\\
\kappa_{\pm,0} &= \frac{1\pm\cos\Theta}{2}D_\downarrow^{(+)}\left(\epsilon_\pm-\epsilon_0+\frac{\Omega}{2}\right)\\
&\quad + \frac{1\mp\cos\Theta}{2}D_\uparrow^{(+)}\left(\epsilon_\pm-\epsilon_0-\frac{\Omega}{2}\right). \qquad \text{(A26b)}
\end{aligned}
$$

The corresponding dispersion functions $D_\sigma^\pm(\omega)$ can be found in Eq. (A20).

All the terms in the last six lines of Eq. (A23) are oscillating in time. They originate purely from the nonsecular treatment, where we also find some $\boldsymbol{\chi}$-dependent terms. These terms also have important roles to play in energy and particle exchange between the QD and side reservoir. The $\boldsymbol{\chi}$-dependent coefficients read

$$
\begin{aligned}
\Upsilon_{0,\pm}(\boldsymbol{\chi}) &= \Upsilon_{0,\pm}^{(\downarrow)} e^{+\mathrm{i}(\epsilon_\pm-\epsilon_0+\frac{\Omega}{2})\chi_{2\downarrow}+\mathrm{i}\chi_{1\downarrow}}\\
&\quad - \Upsilon_{0,\pm}^{(\uparrow)} e^{+\mathrm{i}(\epsilon_\pm-\epsilon_0-\frac{\Omega}{2})\chi_{2\uparrow}+\mathrm{i}\chi_{1\uparrow}}, \qquad \text{(A27a)}\\
\Upsilon_{\pm,0}(\boldsymbol{\chi}) &= \Upsilon_{\pm,0}^{(\downarrow)} e^{-\mathrm{i}(\epsilon_\pm-\epsilon_0+\frac{\Omega}{2})\chi_{2\downarrow}-\mathrm{i}\chi_{1\downarrow}}\\
&\quad - \Upsilon_{\pm,0}^{(\uparrow)} e^{-\mathrm{i}(\epsilon_\pm-\epsilon_0-\frac{\Omega}{2})\chi_{2\uparrow}-\mathrm{i}\chi_{1\uparrow}}, \qquad \text{(A27b)}\\
\xi_{0,\pm}(\boldsymbol{\chi}) &= \xi_{0,\pm}^{(\downarrow)} e^{+\mathrm{i}(\epsilon_\pm-\epsilon_0+\frac{\Omega}{2})\chi_{2\downarrow}+\mathrm{i}\chi_{1\downarrow}}\\
&\quad - \xi_{0,\pm}^{(\uparrow)} e^{+\mathrm{i}(\epsilon_\pm-\epsilon_0-\frac{\Omega}{2})\chi_{2\uparrow}+\mathrm{i}\chi_{1\uparrow}}, \qquad \text{(A27c)}\\
\xi_{\pm,0}(\boldsymbol{\chi}) &= \xi_{\pm,0}^{(\downarrow)} e^{-\mathrm{i}(\epsilon_\pm-\epsilon_0+\frac{\Omega}{2})\chi_{2\downarrow}-\mathrm{i}\chi_{1\downarrow}}\\
&\quad - \xi_{\pm,0}^{(\uparrow)} e^{-\mathrm{i}(\epsilon_\pm-\epsilon_0-\frac{\Omega}{2})\chi_{2\uparrow}-\mathrm{i}\chi_{1\uparrow}}, \qquad \text{(A27d)}
\end{aligned}
$$

where the individual spin-dependent components are given by

$$
\begin{aligned}
\Upsilon_{0,\pm}^{(\downarrow)} &= \frac{\sin\Theta}{4}\Gamma_\downarrow^{(-)}\left(\epsilon_\pm-\epsilon_0+\frac{\Omega}{2}\right), \qquad \text{(A28a)}\\
\Upsilon_{0,\pm}^{(\uparrow)} &= \frac{\sin\Theta}{4}\Gamma_\uparrow^{(-)}\left(\epsilon_\pm-\epsilon_0-\frac{\Omega}{2}\right), \qquad \text{(A28b)}\\
\Upsilon_{\pm,0}^{(\downarrow)} &= \frac{\sin\Theta}{4}\Gamma_\downarrow^{(+)}\left(\epsilon_\pm-\epsilon_0+\frac{\Omega}{2}\right), \qquad \text{(A28c)}\\
\Upsilon_{\pm,0}^{(\uparrow)} &= \frac{\sin\Theta}{4}\Gamma_\uparrow^{(+)}\left(\epsilon_\pm-\epsilon_0-\frac{\Omega}{2}\right), \qquad \text{(A28d)}\\
\xi_{0,\pm}^{(\downarrow)} &= \frac{\sin\Theta}{4}D_\downarrow^{(-)}\left(\epsilon_\pm-\epsilon_0+\frac{\Omega}{2}\right), \qquad \text{(A28e)}\\
\xi_{0,\pm}^{(\uparrow)} &= \frac{\sin\Theta}{4}D_\uparrow^{(-)}\left(\epsilon_\pm-\epsilon_0-\frac{\Omega}{2}\right), \qquad \text{(A28f)}\\
\xi_{\pm,0}^{(\downarrow)} &= \frac{\sin\Theta}{4}D_\downarrow^{(+)}\left(\epsilon_\pm-\epsilon_0+\frac{\Omega}{2}\right), \qquad \text{(A28g)}\\
\xi_{\pm,0}^{(\uparrow)} &= \frac{\sin\Theta}{4}D_\uparrow^{(+)}\left(\epsilon_\pm-\epsilon_0-\frac{\Omega}{2}\right). \qquad \text{(A28h)}
\end{aligned}
$$

In the case when all the terms in the last six lines of Eq. (A23) are oscillating fast, the effects of these terms will very rapidly average to zero. It is then justified to apply the secular approximation to drop these fast oscillating terms. By further setting $\boldsymbol{\chi} = \mathbf{0}$, one will arrive at a Lindblad quantum master equation such that the populations and coherences are dynamically decoupled [66,82]. All the thermodynamics can be analyzed in analogy to that for time-independent situations. By comparing the quasienergies ϵ_+ and ϵ_- in Eq. (A10), one readily finds that fast oscillations only take place in the limit

where the Rabi frequency is much larger than the dissipation strength.

In this work, our investigation is based on the GQME beyond the secular approximation, such that our thermodynamic analysis is valid for a wide range of Rabi frequencies. In particular, we will reveal the essential roles that the nonsecular treatment will play in the thermodynamics of the ESR pumped QD device. Finally, by converting from the interaction picture back into Schrödinger's picture, we arrives at the GQME in the Floquet basis in Eq. (16).

[1] U. Weiss, *Quantum Dissipative Systems*, 3rd ed. (World Scientific, Singapore, 2008).

[2] J. Gemmer, M. Michel, and G. Mahler, *Quantum Thermodynamics: Emergence of Thermodynamic Behavior within Composite Quantum Systems*, Lecture Notes in Physics, 2nd ed. (Springer, Berlin, 2009).

[3] K. Sekimoto, *Stochastic Energetics* (Springer, New York, 2010).

[4] M. Campisi, P. Hänggi, and P. Talkner, Rev. Mod. Phys. **83**, 771 (2011).

[5] U. Seifert, Rep. Prog. Phys. **75**, 126001 (2012).

[6] M. Esposito, M. A. Ochoa, and M. Galperin, Phys. Rev. Lett. **114**, 080602 (2015).

[7] S. Vinjanampathy and J. Anders, Contemp. Phys. **57**, 545 (2016).

[8] J. Anders and M. Esposito, New J. Phys. **19**, 010201 (2017).

[9] M. Carrega, P. Solinas, M. Sassetti, and U. Weiss, Phys. Rev. Lett. **116**, 240403 (2016).

[10] R. Alicki and R. Kosloff, Introduction to quantum thermodynamics: History and prospects, in *Thermodynamics in the Quantum Regime*, edited by F. Binder, L. Correa, C. Gogolin, J. Anders, and G. Adesso, Fundamental Theories of Physics, Vol. 195 (Springer, Cham, 2019).

[11] G. Benenti, G. Casati, K. Saito, and R. S. Whitney, Phys. Rep. **694**, 1 (2017).

[12] R. Kosloff and A. Levy, Annu. Rev. Phys. Chem. **65**, 365 (2014).

[13] R. Uzdin, A. Levy, and R. Kosloff, Phys. Rev. X **5**, 031044 (2015).

[14] B. Leggio and M. Antezza, Phys. Rev. E **93**, 022122 (2016).

[15] J. Roßnagel, S. T. Dawkins, K. N. Tolazzi, O. Abah, E. Lutz, F. Schmidt-Kaler, and K. Singer, Science **352**, 325 (2016).

[16] A. Argun, J. Soni, L. Dabelow, S. Bo, G. Pesce, R. Eichhorn, and G. Volpe, Phys. Rev. E **96**, 052106 (2017).

[17] A. Roulet, S. Nimmrichter, J. M. Arrazola, S. Seah, and V. Scarani, Phys. Rev. E **95**, 062131 (2017).

[18] B. Reid, S. Pigeon, M. Antezza, and G. D. Chiara, Europhys. Lett. **120**, 60006 (2017).

[19] S. Scopa, G. T. Landi, and D. Karevski, Phys. Rev. A **97**, 062121 (2018).

[20] A. Hewgill, A. Ferraro, and G. De Chiara, Phys. Rev. A **98**, 042102 (2018).

[21] J. Goold, M. Huber, A. Riera, L. del Rio, and P. Skrzypczyk, J. Phys. A: Math. Theor. **49**, 143001 (2016).

[22] M. Esposito, U. Harbola, and S. Mukamel, Rev. Mod. Phys. **81**, 1665 (2009).

[23] C. V. den Broeck, Nat. Phys. **6**, 937 (2010).

[24] A. Bérut, A. Arakelyan, A. Petrosyan, S. Ciliberto, R. Dillenschneider, and E. Lutz, Nature (London) **483**, 187 (2012).

[25] M. Esposito and G. Schaller, Europhys. Lett. **99**, 30003 (2012).

[26] A. C. Barato and U. Seifert, Phys. Rev. Lett. **112**, 090601 (2014).

[27] J. M. R. Parrondo, J. M. Horowitz, and T. Sagawa, Nat. Phys. **11**, 131 (2015).

[28] S. Goldt and U. Seifert, Phys. Rev. Lett. **118**, 010601 (2017).

[29] P. Strasberg, G. Schaller, T. Brandes, and M. Esposito, Phys. Rev. X **7**, 021003 (2017).

[30] S. Ito, Phys. Rev. Lett. **121**, 030605 (2018).

[31] S. Toyabe, T. Sagawa, M. Ueda, E. Muneyuki, and M. Sano, Nat. Phys. **6**, 988 (2010).

[32] J. P. Pekola, Nat. Phys. **11**, 118 (2015).

[33] J. Pekola and I. Khaymovich, Ann. Rev. Condens. Matter Phys. **10**, 193 (2019).

[34] O.-P. Saira, Y. Yoon, T. Tanttu, M. Möttönen, D. V. Averin, and J. P. Pekola, Phys. Rev. Lett. **109**, 180601 (2012).

[35] J. V. Koski, V. F. Maisi, T. Sagawa, and J. P. Pekola, Phys. Rev. Lett. **113**, 030601 (2014).

[36] N. Cottet, S. Jezouin, L. Bretheau, P. Campagne-Ibarcq, Q. Ficheux, J. Anders, A. Auffèves, R. Azouit, P. Rouchon, and B. Huard, Proc. Natl. Acad. Sci. **114**, 7561 (2017).

[37] Y. Masuyama, K. Funo, Y. Murashita, A. Noguchi, S. Kono, Y. Tabuchi, R. Yamazaki, M. Ueda, and Y. Nakamura, Nat. Commun. **9**, 1291 (2018).

[38] J. V. Koski, V. F. Maisi, J. P. Pekola, and D. V. Averin, Proc. Natl. Acad. Sci. **111**, 13786 (2014).

[39] N. Bar-Gill, L. M. Pham, A. Jarmola, D. Budker, and R. L. Walsworth, Nat. Commun. **4**, 1743 (2013).

[40] J. W. Park, Z. Z. Yan, H. Loh, S. A. Will, and M. W. Zwierlein, Science **357**, 372 (2017).

[41] I. Žutić, J. Fabian, and S. D. Sarma, Rev. Mod. Phys. **76**, 323 (2004).

[42] D. D. Awschalom, L. C. Bassett, A. S. Dzurak, E. L. Hu, and J. R. Petta, Science **339**, 1174 (2013).

[43] M. Xiao, I. Martin, E. Yablonovitch, and H. Jiang, Nature (London) **430**, 435 (2004).

[44] J. M. Elzerman, R. Hanson, L. H. W. van Beveren, B. Witkamp, L. M. K. Vandersypen, and L. P. Kouwenhoven, Nature (London) **430**, 431 (2004).

[45] Y. M. Blanter and M. Büttiker, Phys. Rep. **336**, 1 (2000).

[46] Y. V. Nazarov (ed.), *Quantum Noise in Mesoscopic Physics* (Kluwer Academic Publishers, Dordrecht, 2003).

[47] D. W. Hone, R. Ketzmerick, and W. Kohn, Phys. Rev. E **79**, 051129 (2009).

[48] J. H. Shirley, Phys. Rev. **138**, B979 (1965).

[49] M. Holthaus and B. Just, Phys. Rev. A **49**, 1950 (1994).

[50] M. Grifoni and P. Hänggi, Phys. Rep. **304**, 229 (1998).

[51] K. Szczygielski, D. Gelbwaser-Klimovsky, and R. Alicki, Phys. Rev. E **87**, 012120 (2013).

[52] J. König and J. Martinek, Phys. Rev. Lett. **90**, 166602 (2003).

[53] P. Stegmann, J. König, and S. Weiss, Phys. Rev. B **98**, 035409 (2018).
[54] M. G. Schultz and F. von Oppen, Phys. Rev. B **80**, 033302 (2009).
[55] H. P. Breuer and F. Petruccione, *The Theory of Open Quantum Systems* (Oxford University Press, New York, 2002).
[56] H. Spohn, Rev. Mod. Phys. **52**, 569 (1980).
[57] D. A. Bagrets and Y. V. Nazarov, Phys. Rev. B **67**, 085316 (2003).
[58] J. Y. Luo, H. J. Jiao, J. Hu, X.-L. He, X. L. Lang, and S.-K. Wang, Phys. Rev. B **92**, 045107 (2015).
[59] N. Ubbelohde, C. Fricke, F. Hohls, and R. J. Haug, Phys. Rev. B **88**, 041304(R) (2013).
[60] D. Urban and J. König, Phys. Rev. B **79**, 165319 (2009).
[61] R.-Q. Wang, L. Sheng, L.-B. Hu, B. G. Wang, and D. Y. Xing, Phys. Rev. B **84**, 115304 (2011).
[62] J. Y. Luo, Y. Yan, Y. Huang, L. Yu, X.-L. He, and H. J. Jiao, Phys. Rev. B **95**, 035154 (2017).
[63] M. J. Stevens, A. L. Smirl, R. D. R. Bhat, A. Najmaie, J. E. Sipe, and H. M. van Driel, Phys. Rev. Lett. **90**, 136603 (2003).
[64] J. Hübner, W. W. Rühle, M. Klude, D. Hommel, R. D. R. Bhat, J. E. Sipe, and H. M. van Driel, Phys. Rev. Lett. **90**, 216601 (2003).
[65] F. W. J. Hekking and J. P. Pekola, Phys. Rev. Lett. **111**, 093602 (2013).
[66] M. Silaev, T. T. Heikkilä, and P. Virtanen, Phys. Rev. E **90**, 022103 (2014).
[67] P. Solinas, D. V. Averin, and J. P. Pekola, Phys. Rev. B **87**, 060508(R) (2013).
[68] S. Gasparinetti, P. Solinas, A. Braggio, and M. Sassetti, New J. Phys. **16**, 115001 (2014).
[69] D. Kondepudi and I. Prigogine, *Modern Thermodynamics* (Wiley, New York, 1998).
[70] S. R. de Groot and P. Mazur, *Non-Equilibrium Thermodynamics* (Dover, New York, 1984).
[71] I. Prigogine and G. Nicolis, *Self-Organization in Non-Equilibrium Systems* (Wiley, New York, 1977).
[72] P. Gaspard, Physica A: Stat. Mech. Appl. **369**, 201 (2006).
[73] Y. J. Yan and R. X. Xu, Annu. Rev. Phys. Chem. **56**, 187 (2005).
[74] R. X. Xu and Y. J. Yan, J. Chem. Phys. **116**, 9196 (2002).
[75] B. Wunsch, M. Braun, J. König, and D. Pfannkuche, Phys. Rev. B **72**, 205319 (2005).
[76] J. Y. Luo, H. J. Jiao, Y. Shen, G. Cen, X.-L. He, and C. Wang, J. Phys.: Condens. Matter **23**, 145301 (2011).
[77] J. Y. Luo, Y. Shen, X.-L. He, X.-Q. Li, and Y. J. Yan, Phys. Lett. A **376**, 59 (2011).
[78] J. König and Y. Gefen, Phys. Rev. B **65**, 045316 (2002).
[79] F. Marquardt and C. Bruder, Phys. Rev. B **68**, 195305 (2003).
[80] J. Y. Luo, H. J. Jiao, F. Li, X.-Q. Li, and Y. J. Yan, J. Phys.: Condens. Matter **21**, 385801 (2009).
[81] J. Y. Luo, H. J. Jiao, J. Z. Wang, Y. Shen, and X.-L. He, Phys. Lett. A **374**, 4904 (2010).
[82] G. B. Cuetara, A. Engel, and M. Esposito, New J. Phys. **17**, 055002 (2015).